Mosaic Attenuation: Etiology, Methods of Differentiation, and Pitfalls[1]

Seth J. Kligerman, MD
Travis Henry, MD
Cheng T. Lin, MD
Teri J. Franks, MD
Jeffrey R. Galvin, MD

Abbreviations: CTEPH = chronic thromboembolic pulmonary hypertension, DIPNECH = diffuse idiopathic pulmonary neuroendocrine cell hyperplasia, H-E = hematoxylin-eosin, PAH = pulmonary arterial hypertension, PCH = pulmonary capillary hemangiomatosis, PVOD = pulmonary veno-occlusive disease

RadioGraphics 2015; 35:1360–1380

Published online 10.1148/rg.2015140308

Content Codes: CH CT

[1]From the Department of Radiology and Nuclear Medicine, University of Maryland School of Medicine, 22 S Greene St, Baltimore, MD 21201 (S.J.K., C.T.L., J.R.G.); Department of Radiology and Imaging Sciences, Emory University School of Medicine, Atlanta, Ga (T.H.); and Division of Pulmonary and Mediastinal Pathology, The Joint Pathology Center, Defense Health Agency, National Capital Region Medical Directorate, Silver Spring, Md (T.J.F.). Presented as an education exhibit at the 2013 RSNA Annual Meeting. Received September 30, 2014; revision requested December 1 and received January 22, 2015; accepted January 23. For this journal-based SA-CME activity, the authors, editor, and reviewers have disclosed no relevant relationships. **Address correspondence to** S.J.K. (e-mail: *skligerman@umm.edu*).

SA-CME LEARNING OBJECTIVES

After completing this journal-based SA-CME activity, participants will be able to:

- Describe the various causes of a mosaic attenuation pattern on thoracic CT.
- Discuss differentiation of airway causes of mosaic attenuation from vascular causes.
- Identify ancillary findings of mosaic attenuation on thoracic CT to help narrow the differential diagnosis.

See www.rsna.org/education/search/RG.

Mosaic attenuation is a commonly encountered pattern on computed tomography that is defined as heterogeneous areas of differing lung attenuation. This heterogeneous pattern of attenuation is the result of diverse causes that include diseases of the small airways, pulmonary vasculature, alveoli, and interstitium, alone or in combination. Small airways disease can be a primary disorder, such as respiratory bronchiolitis or constrictive bronchiolitis, or be part of parenchymal lung disease, such as hypersensitivity pneumonitis, or large airways disease, such as bronchiectasis and asthma. Vascular causes resulting in mosaic attenuation are typically chronic thromboembolic pulmonary hypertension, which is characterized by organizing thrombi in the elastic pulmonary arteries, or pulmonary arterial hypertension, a heterogeneous group of diseases affecting the distal pulmonary arterioles. Diffuse ground-glass opacity can result in a mosaic pattern related to a number of processes in acute (eg, infection, pulmonary edema), subacute (eg, organizing pneumonia), or chronic (eg, fibrotic diseases) settings. Imaging clues that can assist the radiologist in pinpointing a diagnosis include evidence of large airway involvement, cardiovascular abnormalities, septal thickening, signs of fibrosis, and demonstration of airtrapping at expiratory imaging.

Introduction

Mosaic attenuation is an imaging pattern on computed tomography (CT) of the chest that is defined as variable lung attenuation that results in a heterogeneous appearance of the parenchyma. It is important to remember that mosaic attenuation is a finding that implies a large differential diagnosis and is not a diagnosis in itself. Although the differential diagnosis is broad, mosaic attenuation most commonly occurs in diseases that affect the small airways, pulmonary vasculature, alveoli, and interstitium, alone or in combination.

Small airways disease can be a primary disorder, such as respiratory bronchiolitis or constrictive bronchiolitis, or be part of parenchymal lung disease, such as hypersensitivity pneumonitis, or large airways disease, such as bronchiectasis and asthma (1). Although the predominant cause of mosaic attenuation may vary by institution, parenchymal lung diseases contribute to approximately one-half of cases of mosaic attenuation, whereas diseases of the small airways are the underlying cause in approximately one-third of cases (2,3). Diseases of the pulmonary vasculature contribute to the remaining cases.

The major difficulty with this pattern lies in the fact that it can be difficult for a radiologist to determine which areas of lung attenuation are normal and which are abnormal. In some instances, the areas

TEACHING POINTS

- One of the best methods to differentiate between causes of mosaic attenuation is to perform expiratory imaging.
- The distribution of bronchiectasis can help differentiate between small airways and parenchymal causes.
- Direct visualization of the small airways is not possible on CT in normal individuals. Therefore, the presence of centrilobular nodules on CT in conjunction with mosaic attenuation is a good clue that injury to the small airways is the cause of the mosaicism.
- The size and morphology of the central and peripheral pulmonary arteries are helpful clues to differentiate vascular causes of mosaic attenuation from small airways disease and ground-glass opacity. The presence of enlarged pulmonary arteries should prompt evaluation for pulmonary hypertension as a cause of mosaic attenuation.
- The presence of diffuse ground-glass opacity with superimposed interlobular septal thickening is seen in only a few disease states and can help narrow the differential diagnosis of a mosaic pattern. Patient history can further help narrow the differential diagnosis.

of lower attenuation are abnormal, while in other instances the areas of higher attenuation are abnormal. In certain diseases, areas of both high and low attenuation are abnormal, making it difficult to determine if normal lung parenchyma exists.

The purpose of this article is to review the causes of a mosaic attenuation pattern and highlight distinguishing features that can help one determine the underlying pathologic process.

Mosaic Attenuation and Airtrapping: How Much Is Normal?

Some degree of parenchymal heterogeneity can be seen in normal individuals. In general, the most dependent portions of the lung are of slightly higher attenuation than the less-dependent lung. However, discontinuity of this gradient can be seen at the level of the fissures, where the posterior aspects of the upper lobe often have higher attenuation than the superior segments of the lower lobes (4). In addition, perfusion gradients exist axially, with an increased degree of perfusion centrally than peripherally. However, even when these physiologic gradients are taken into account, mild mosaic attenuation at inspiration can be seen in up to 20% of normal patients (5). This degree of heterogeneity may be further accentuated at imaging performed below total lung capacity.

One of the best methods to differentiate between causes of mosaic attenuation is to perform expiratory imaging. In patients with small airways disease, air cannot readily escape in the regions where the small airways are obstructed. Because of this, the attenuation of the involved segments remains relatively unchanged in comparison with that at inspiratory imaging. With air normally conducting through the noninvolved areas, the difference in attenuation between the normal and abnormal areas becomes much more pronounced and airtrapping can be diagnosed (Fig 1). At expiratory CT in patients without small airways disease, the lungs should show a relatively diffuse increase in attenuation and appear grayer (Fig 2).

As with inspiratory imaging, a normal gradient exists at expiratory imaging, with the dependent lung having slightly higher attenuation than the nondependent lung (6). However, beyond this physiologic gradient, areas of lobular airtrapping occur in 40%–80% of normal patients on both qualitative and quantitative CT (Fig 3) (4,5,7–9). In a study by Park et al (5), mild (total area < three adjacent lobules) and moderate (area between three lobules and a pulmonary segment) airtrapping occurred to a similar degree in normal individuals with normal pulmonary function test results and patients with asthma.

In addition, airtrapping involving an entire pulmonary segment can occasionally be seen in a small percentage of normal individuals, and the presence of airtrapping increases with age and is more pronounced in smokers (4,10,11). Therefore, various degrees of mosaicism and airtrapping may be an incidental finding and not related to the underlying symptoms of the patient. In general, mosaic attenuation or airtrapping involving more than a pulmonary segment often has an underlying pathologic basis for which a cause should be sought.

Etiology

Small Airways Disease

Small airways are defined as noncartilaginous airways with an internal diameter of less than 2 mm and are located from approximately the eighth generation of airways down to the terminal bronchioles (smallest airways without alveoli) and respiratory bronchioles (airways distal to terminal bronchioles that partake in gas exchange) (12). In normal patients, these small airways are not visible on CT due to their small size (13). However, in certain instances, these small airways may become visible due to underlying disease.

Numerous classification systems have been used to describe small airways diseases based on clinical, imaging, and histologic findings. On a practical basis, small airways disease can be classified as a primary bronchiolar disorder, which includes constrictive bronchiolitis, cellular bronchiolitis, diffuse panbronchiolitis, respiratory bronchiolitis, mineral dust airways disease, and follicular bronchiolitis; bronchiolar involvement in diffuse interstitial lung disease, such as hypersensitivity pneumonitis; and bronchiolar involvement in large airways disease, such as bronchiectasis or asthma (1) (Table 1).

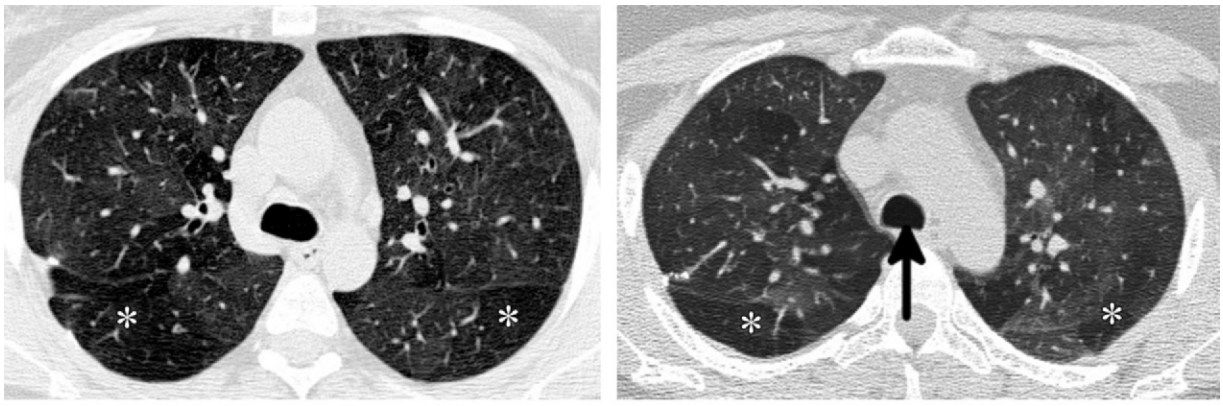

a. b.

Figure 1. Airtrapping due to constrictive bronchiolitis in a 43-year-old woman with rheumatoid arthritis. **(a)** Axial CT image at the level of the carina shows mosaic attenuation, with geographic areas of decreased attenuation (*) adjacent to normal lung. Note the relative decrease in vascularity in the hypoattenuated regions, a finding seen in both small airways disease and vascular causes of mosaic attenuation. **(b)** Expiratory CT image at a similar level shows that the areas of hypoattenuated lung in **a** have not changed in attenuation due to airtrapping (*). The adjacent areas of higher-attenuation lung represent the expected increase in attenuation at expiratory imaging. Bowing of the posterior wall of the trachea (arrow) signifies good expiratory effort. The presence of airtrapping confirms a small airways disease cause of the mosaic attenuation.

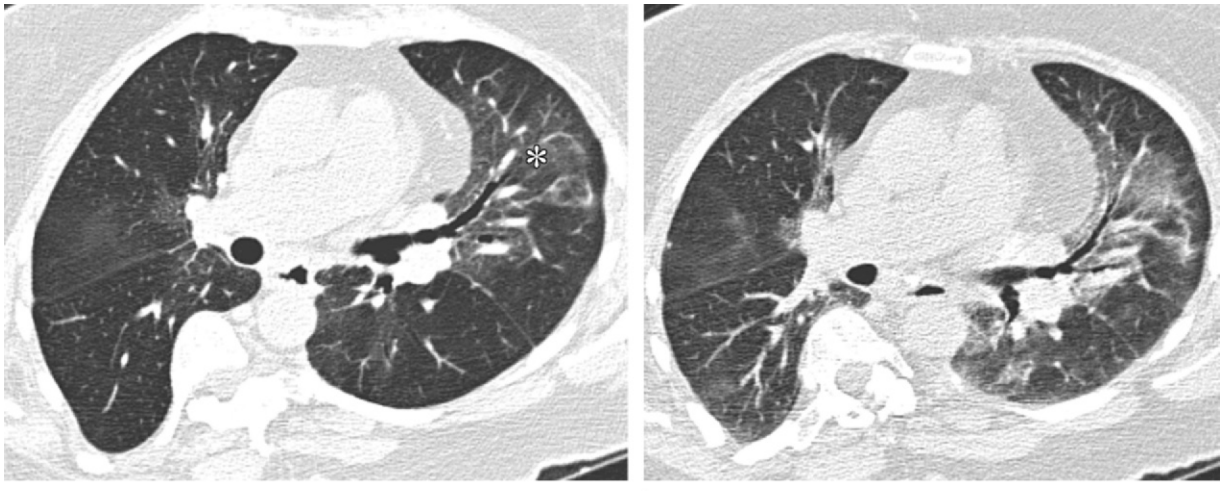

a. b.

Figure 2. Inspiratory and expiratory CT in a 55-year-old woman with organizing pneumonia. **(a)** Axial CT image during inspiration shows mosaic attenuation, with slightly increased attenuation most prominent in the left upper lobe (*). **(b)** Expiratory CT image at the same level shows a diffuse increase in attenuation in both the areas of relatively increased attenuation and the areas of relatively decreased attenuation. This finding allows exclusion of airtrapping, and the similar size of the pulmonary vasculature throughout the lung suggests that the area of increased attenuation is abnormal. Subsequent biopsy of this region demonstrated organizing pneumonia.

Inflammatory small airways disease can be categorized by the underlying pathologic process. Causes of small airways inflammation are many and include infection (cellular bronchiolitis), cigarette smoking (respiratory bronchiolitis), inhalation of organic or inorganic antigens (hypersensitivity pneumonitis or mineral dust airways disease), and lymphoid hyperplasia (follicular bronchiolitis) (10,14–17). Although small airway inflammation can lead to permanent obstruction of the small airways, it is often a reversible process.

In contrast, the submucosal and peribronchiolar fibrosis of constrictive bronchiolitis leads to irreversible obstruction of the small airways (Table 2) (18). Inflammation and/or constriction or obliteration of the small airways is a common pathologic process and leads to both direct and indirect signs of the underlying disease state (Fig 4) (19).

Pulmonary Vascular Disease

Primary pulmonary vascular disease results in mosaic attenuation due to regional differences in lung perfusion. Mosaic attenuation is most commonly seen in association with pulmonary hypertension, which will lead to enlargement of the pulmonary trunk and remodeling of the right heart, including right ventricular enlargement

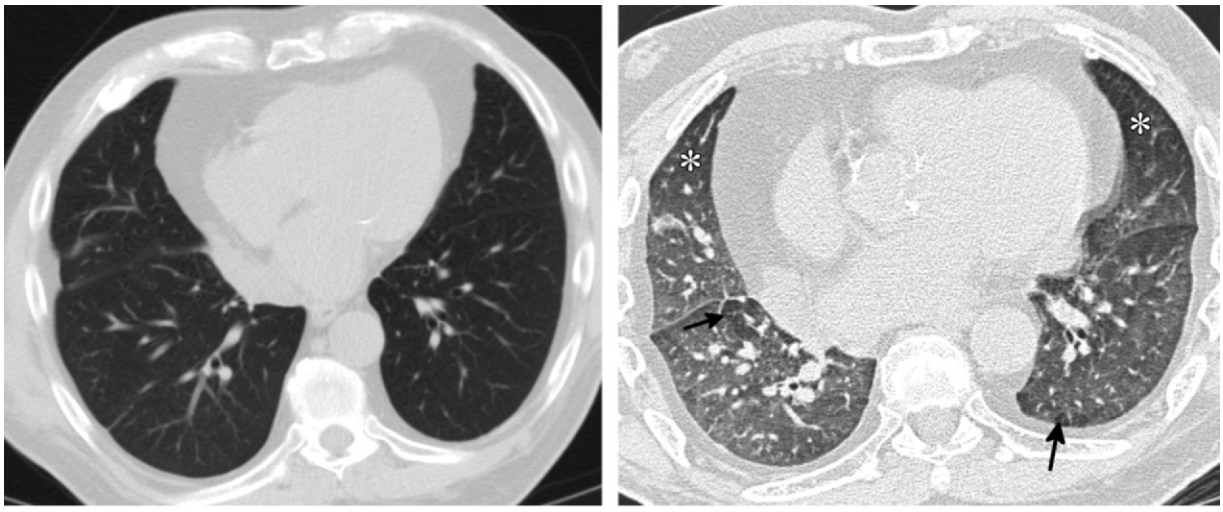

a. b.

Figure 3. Normal variation in lung attenuation at expiration in a 73-year-old woman with a history of ulcerative colitis and worsening shortness of breath. **(a)** Inspiratory CT image shows normal lung attenuation. **(b)** High-resolution CT image during expiration shows the normal physiologic gradient, with the anterior portion of the lung (*) having lower attenuation than the posterior portion. The dependent portion of the lung demonstrates heterogeneous parenchyma at expiration, although almost all of the lung has increased in attenuation. In addition, there are a few dependent lobules that remain lucent (arrows). This variation at expiratory imaging is seen in a large percentage of patients and is considered to be nonpathologic.

Table 1: Classification of Bronchiolar Disorders

Primary bronchiolar disorders
Constrictive bronchiolitis
Acute bronchiolitis
Diffuse panbronchiolitis
Respiratory bronchiolitis
Mineral dust airways disease
Follicular bronchiolitis
Interstitial lung disease with prominent bronchiolar involvement
Hypersensitivity pneumonitis
Respiratory bronchiolitis–interstitial lung disease
Desquamative interstitial pneumonia
Organizing pneumonia
Bronchiolar involvement in large airways disease
Chronic bronchitis
Asthma
Bronchiectasis

and hypertrophy (20). Although any cause of pulmonary hypertension can lead to mosaic attenuation, chronic thromboembolic pulmonary hypertension (CTEPH) and primary pulmonary arterial hypertension (PAH) (previously referred to as primary pulmonary hypertension), are the most common vascular causes of this finding (3).

However, mosaicism can also be seen in patients with pulmonary hypertension due to longstanding cardiac shunts (21). Pulmonary hypertension due to left heart disease or lung disease and/or hypoxia are less likely causes of a mosaic pattern (21). These can usually be identified at imaging by the presence of ancillary findings (eg, dilated left heart; septal thickening; presence of severe emphysema or fibrosis).

Pulmonary veno-occlusive disease (PVOD) and pulmonary capillary hemangiomatosis (PCH) can also lead to mosaic attenuation but are rare and are associated with additional parenchymal findings (discussed later). Vasculitis can also lead to mosaic attenuation, but this is often due to increased ground-glass opacity from areas of pulmonary hemorrhage and is also discussed separately (22).

Ground-Glass Opacity

At CT, ground-glass opacity occurs when there is increased lung attenuation through which the underlying airway and vessels remain visible (23). Diffuse ground-glass opacity is a nonspecific finding with numerous causes (Table 3). In many cases, it may be easy to distinguish the abnormally high-attenuation lung from normal surrounding lung parenchyma, but in other cases differentiation of normal lower-attenuation parenchyma from increased ground-glass opacity can be difficult. However, there are certain findings (discussed later) that can help differentiate between the different causes and narrow the differential diagnosis.

Pathophysiology

Small Airways Disease

Mosaic attenuation can be an indirect sign of small airways disease on inspiratory CT. Although mosaic attenuation is a nonspecific finding, small airway causes of mosaicism are more common than vascular causes (24). In patients with small

airways disease, mosaic attenuation is due to the presence of normally attenuated lung in direct apposition to abnormal hyperlucent lung.

Although bronchiolar obstruction is present, the lung distal to the obstruction remains aerated through interalveolar (pores of Kohn), bronchiolar-alveolar (canals of Lambert), and interbronchiolar (channels of Martin) communications (25). Despite aeration though collateral airflow, obstruction of the small airways reduces the ability of the involved lung to perform adequate gas exchange, and blood is shunted away from the areas of obstruction (3). This shunting of blood leads to decreased perfusion in the areas with small airways disease and also contributes to the more lucent appearance. The shunting of blood away from these areas leads to decreased size of the vasculature in the hyperlucent lung, a finding also seen in many vascular causes of mosaic attenuation.

Depending on the type and degree of injury, the mosaicism can be focal or diffuse and the extent of abnormality can vary dramatically. In some cases, the degree of small airway injury is so diffuse that it can be difficult to locate normal parenchyma (Fig 5). Although small airways disease is the most common cause of mosaic attenuation where the hyperlucent lung is abnormal, disease of the pulmonary vasculature can lead to a similar appearance.

Pulmonary Vascular Disease

In PAH, the primary abnormality is in the distal pulmonary arterioles, whereas in CTEPH organizing thrombi are present in the elastic pulmonary arteries and may cause partial or complete vascular occlusion (26). In these cases, the heterogeneity in parenchymal attenuation reflects decreased blood flow to areas of reduced attenuation (11). On the basis of the presence of mosaic attenuation alone, it can be difficult to differentiate small airways disease from small vessel disease, as both lead to reduced caliber of the vessels in the areas of decreased attenuation (3). Other clues on CT (discussed later) can help one make the correct diagnosis.

Ground-Glass Opacity

Ground-glass opacity is a common finding that occurs when there is increased attenuation that does not obscure the underlying structures of the lung, as seen with consolidation (27). Pathologically, the causes of ground-glass opacity at imaging are numerous and include thickening of the alveolar wall due to inflammation or fibrosis; alveolar collapse; increased capillary blood volume; the presence of fluid, cells, or amorphous material partially filling the alveolar spaces; or a combination of these (23,27–29).

Table 2: Causes of Constrictive Bronchiolitis

Postinfectious
Viral
Mycoplasma
Collage vascular disease
Rheumatoid arthritis
Systemic lupus erythematosus
Systemic sclerosis
Mixed connective tissue disease
Transplantation
Graft-versus-host disease
Allograft transplantation
Drugs
D-penicillamine
Gold
Cocaine
Carmustine
Cryptogenic
Toxic fume exposure
Nitrogen dioxide
Sulfur dioxide
Ammonia
Chlorine
Phosgene
Diacetyl (popcorn workers)
Miscellaneous
Ulcerative colitis
DIPNECH
Stevens-Johnson syndrome
Paraneoplastic pemphigus

Note.—DIPNECH = diffuse idiopathic pulmonary neuroendocrine cell hyperplasia.

Table 3: Causes of Mosaic Attenuation Due to Diffuse Ground-Glass Opacity

Acute causes
Pulmonary edema
Pulmonary hemorrhage
Infections
Pneumocystis pneumonia
Cytomegalovirus pneumonia
Herpes simplex pneumonia
Diffuse alveolar damage, exudative phase
Acute respiratory distress syndrome
Acute interstitial pneumonia
Acute eosinophilic pneumonia
Subacute to chronic causes
Organizing pneumonia
Hypersensitivity pneumonitis
Infections
Pneumocystis pneumonia
Diffuse alveolar damage, organizing and fibrotic phases
Nonspecific interstitial pneumonia

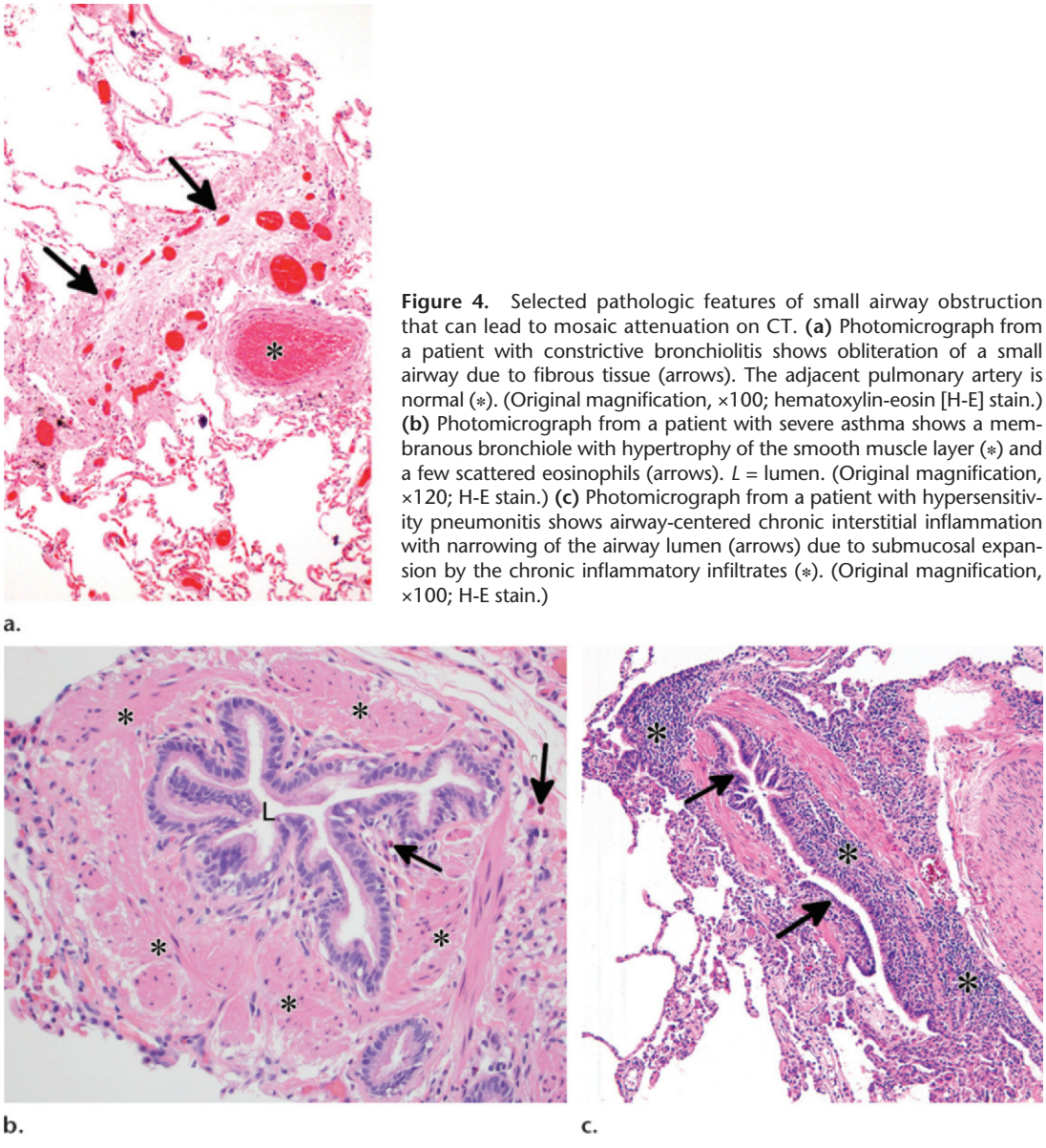

Figure 4. Selected pathologic features of small airway obstruction that can lead to mosaic attenuation on CT. **(a)** Photomicrograph from a patient with constrictive bronchiolitis shows obliteration of a small airway due to fibrous tissue (arrows). The adjacent pulmonary artery is normal (*). (Original magnification, ×100; hematoxylin-eosin [H-E] stain.) **(b)** Photomicrograph from a patient with severe asthma shows a membranous bronchiole with hypertrophy of the smooth muscle layer (*) and a few scattered eosinophils (arrows). *L* = lumen. (Original magnification, ×120; H-E stain.) **(c)** Photomicrograph from a patient with hypersensitivity pneumonitis shows airway-centered chronic interstitial inflammation with narrowing of the airway lumen (arrows) due to submucosal expansion by the chronic inflammatory infiltrates (*). (Original magnification, ×100; H-E stain.)

However, differentiation between interstitial and alveolar causes of ground-glass opacity on imaging is difficult as the imaging appearances overlap. For instance, disease states that initially involve the airspaces, such as pulmonary hemorrhage, often cause development of imaging signs of interstitial abnormalities, such as septal thickening, from the repair and clearance process. Similarly, many causes including infections such as *Pneumocystis jirovecii* pneumonia, diffuse alveolar damage, and organizing pneumonia lead to both interstitial and alveolar abnormalities (30).

Methods of Differentiation

Assess Morphology of Peripheral Pulmonary Vasculature

One of the first steps in determining the cause of mosaic attenuation is to determine which portion of the parenchyma is abnormal. Although in some cases this may be clear, in many cases it can be difficult to separate normal from abnormal parenchyma. One important clue to determining the correct path is to evaluate the size of the peripheral pulmonary arteries in the more lucent lung. With vascular causes, the peripheral pulmonary vasculature is attenuated in areas of decreased attenuation, corresponding to vascular territories where segmental or subsegmental arteries are narrowed or occluded (Fig 6a) (31,32). This finding is classically described in but not limited to CTEPH.

However, this finding can also be seen in cases of small airways disease, where small airway obstruction or fibrosis leads to hypoxic vasoconstriction in the affected lung, shunting blood away from areas of reduced gas exchange (Fig 6b). This results in subsequent hyperperfusion of adjacent normal lung, leading to relative increased attenuation and

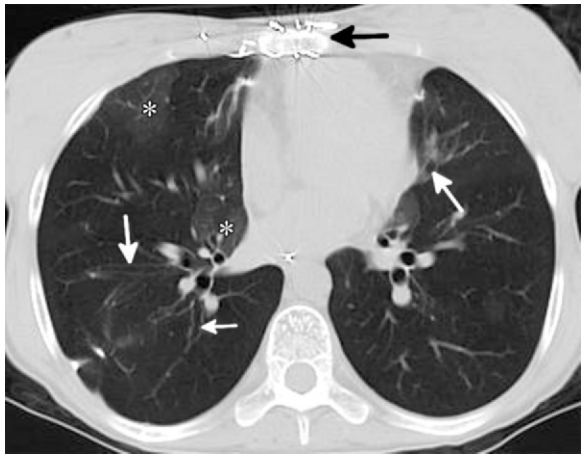

Figure 5. Constrictive bronchiolitis in a 22-year-old woman with a history of lung transplantation for cystic fibrosis. Axial CT image of the lungs shows a near homogeneous appearance. However, on closer inspection, a few areas of slightly higher-attenuation lung are present (*), which represent more normal lung. The large airways (white arrows), although not thickened, do not taper normally and there is no evidence of peripheral fibrosis, suggesting an airways cause. The presence of clamshell median sternotomy wires (black arrow) is a clue to prior lung transplantation and helps support the diagnosis of constrictive bronchiolitis even in the absence of a good clinical history.

areas of ground-glass opacity. Although this finding can be seen in both small airways (Fig 7) and vascular causes, it is often more pronounced in cases of pulmonary hypertension, where the hyperperfused segmental and subsegmental vasculature is often engorged and significantly larger than the adjacent bronchus (Fig 6a).

In cases of ground-glass opacity related to parenchymal lung disease, the size and number of the segmental and subsegmental pulmonary arteries is uniform throughout, which can help differentiate between ground-glass opacity and other causes of mosaic attenuation (Figs 2, 6c). Therefore, attenuation of the peripheral pulmonary vasculature in the lucent lung is an excellent clue that the underlying cause is related to either small airways or vascular disease. However, in some early or mild cases of small airways or vascular disease, this finding may be imperceptible.

Look at the Large Airways

Although small airways disease involves bronchioles below the normal resolution of CT, more proximal abnormalities of the visible bronchi can be a good indicator that the underlying mosaic attenuation is related to small airways disease. These abnormalities range from thickening due to inflammation of the large airways (bronchitis) to distortion and permanent dilatation (bronchiectasis). In a study by Worthy et al (3), the presence of abnormalities of the large airways was the best predictor that the underlying cause of the mosaic attenuation was due to a disease process of the small airways, even better than airtrapping.

In patients with large airways disease, inflammation leads to wall thickening and increased mucus production. Infection, most notably viral infections, is the most common mediator; however, acute airway inflammation can also be seen with inhalational injury secondary to various toxins. Chronic large airways disease is commonly seen in asthmatics or smokers. All of these conditions can lead to injury not only of the large airways but of the small airways as well (Fig 4b). Therefore, CT findings of bronchial wall thickening associated with mild distortion of the airways and associated endobronchial mucus plugging suggest that mosaic attenuation, when present, is secondary to downstream injury to the small airways (Fig 6b, 7a). In addition, bronchial wall thickening can be the result of fluid overload that results in bronchial wall edema or fluid within the connective tissue surrounding the bronchi. Mucus plugging and airway distortion should be absent (Fig 8) (33).

Bronchiectasis, which represents permanent dilatation of the bronchi, can be associated with mosaic attenuation. In many instances, dilatation and damage to the larger airways suggests that the mosaic attenuation is secondary to disease of the small airways, since these diseases can damage both. This includes congenital causes that lead to repeat infection, such as ciliary dyskinesia and cystic fibrosis (Fig 7a), and causes of constrictive bronchiolitis such as prior viral infection (Swyer-James syndrome), toxic inhalational injury, and allogeneic transplantation of the lungs (Fig 5), solid organs, bone marrow, or stem cells (Fig 9).

However, the presence of bronchiectasis alone does not confirm a small airways cause. The distribution of bronchiectasis can help differentiate between small airways and parenchymal causes. In cases of small airways disease, most notably constrictive bronchiolitis, the abnormal bronchi will supply areas of hypoattenuated lung, while more normal-appearing bronchi will be located in areas of more normal parenchymal attenuation (Figs 5, 6b, 7a, 9).

This distribution is in stark contrast to the bronchial dilatation seen in certain parenchymal causes of mosaicism such as organizing pneumonia (Fig 7b), the organizing phase of diffuse alveolar damage, and nonspecific interstitial pneumonia. In these diseases, increased parenchymal attenuation is secondary to interstitial inflammation, interstitial

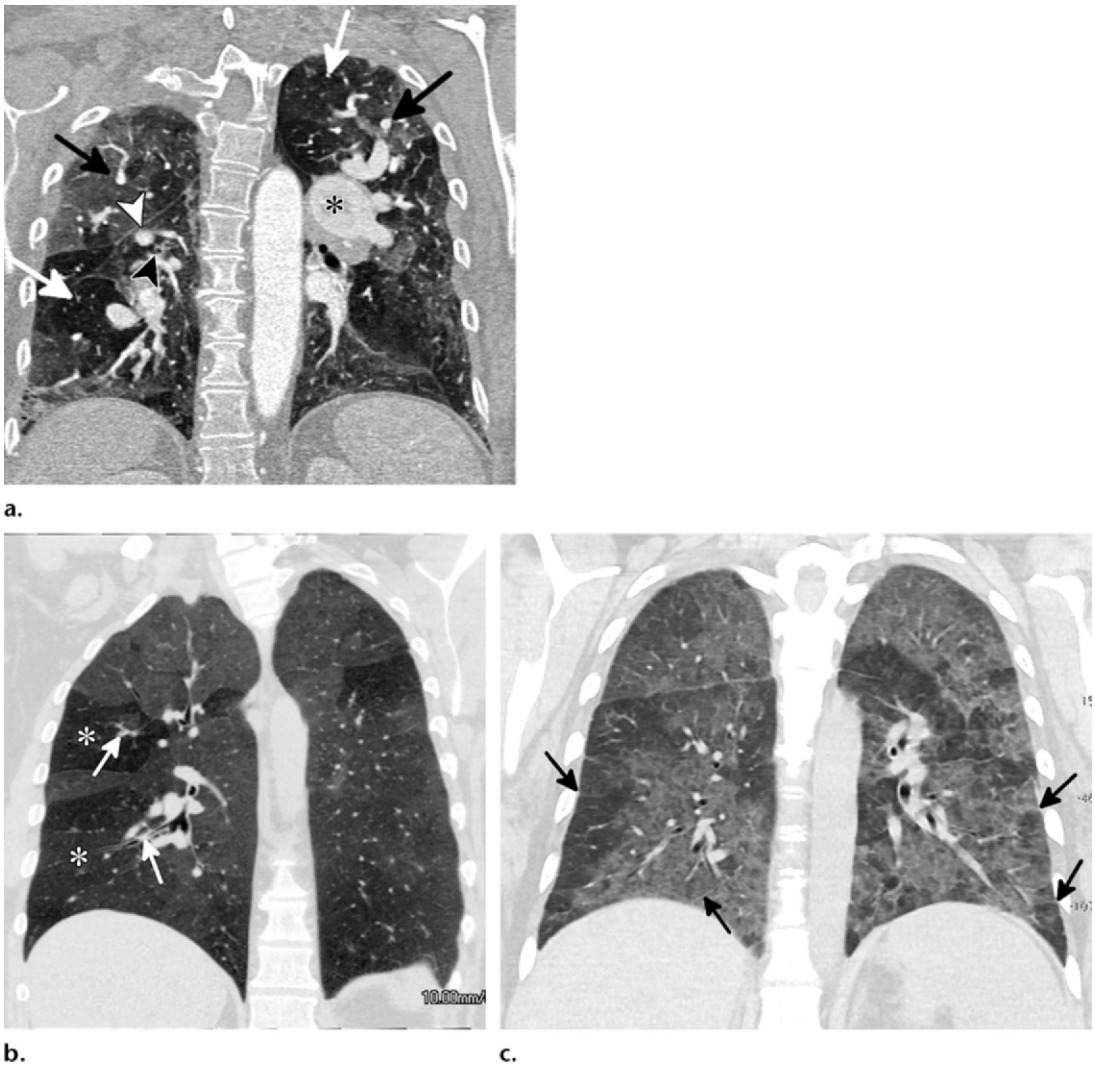

Figure 6. Airway and peripheral pulmonary artery assessment in three patients with mosaic attenuation. **(a)** Mosaic attenuation due to chronic thromboembolic disease in a 48-year-old man. Coronal CT image shows large segmental and subsegmental areas of hypoattenuation due to vascular occlusion adjacent to areas of increased attenuation representing regional hyperperfusion. Note the relative paucity and reduced size of the pulmonary artery segments and subsegments in the areas of decreased attenuation (white arrows) compared with areas of higher attenuation (black arrows). Although this finding can be seen in cases of small airways disease, the right lower lobe segmental pulmonary artery (white arrowhead) is much larger than the associated segmental bronchus (black arrowhead) and the left pulmonary artery is enlarged (*), findings that suggest pulmonary hypertension. **(b)** Mosaic attenuation in a 54-year-old man with chronic cough and poorly controlled asthma. Coronal CT image shows multiple well-defined areas of decreased attenuation throughout both lungs (*). The vasculature in the more lucent lung is attenuated compared with that in the higher-attenuation lung, suggestive of a pathologic process involving that small airway or pulmonary vasculature. Close evaluation shows that the large airways supplying these hyperlucent areas demonstrate endobronchial mucus plugging (arrows), which suggests a more downstream small airways process. **(c)** Mosaic attenuation in a 41-year-old man with diffuse alveolar hemorrhage. Coronal CT image shows mosaic attenuation, with diffuse ground-glass opacity interspersed with areas of normal lung attenuation. There is no vascular attenuation and the airways are normal, both of which suggest a parenchymal cause of mosaic attenuation. Associated septal thickening (arrows) narrows the differential diagnosis to include hemorrhage, edema, *Pneumocystis* pneumonia, and diffuse alveolar damage.

fibrosis, and/or alveolar collapse. Therefore, the dilated airways tend to be most prominent in the areas of increased attenuation and this finding can help in differentiation from small airways causes. Other findings associated with fibrosis, such as reticulation, may be present. The large airway dilatation seen in certain parenchymal diseases such as organizing pneumonia and the organizing phase of diffuse alveolar damage may be transient and can improve or resolve with resolution of the injury. Bronchiectasis is not a common finding in patients with pulmonary hypertension and other vascular causes of mosaic attenuation.

Look for Direct Signs of Small Airway Injury

Direct visualization of the small airways is not possible on CT in normal individuals. Therefore,

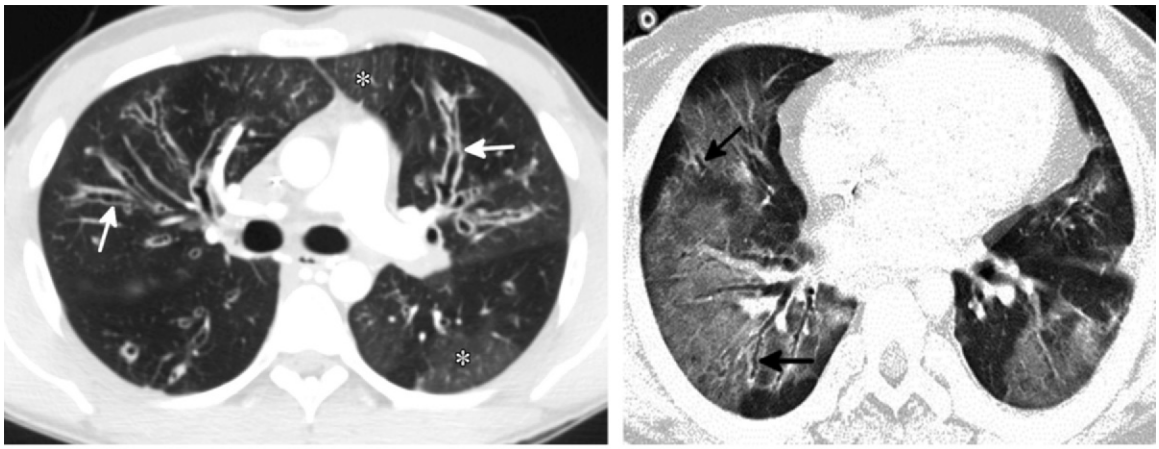

a. b.

Figure 7. Distribution of abnormal airways in two patients with mosaic attenuation. **(a)** Mosaic attenuation in a 22-year-old woman with cystic fibrosis. Axial CT image shows thick-walled bronchiectatic airways, some with associated mucus plugging (arrows). The bronchiectatic airways extend into the more lucent lung due to coexistent small airways disease. The airways in the adjacent lung (*), which has higher attenuation than normal due to hyperperfusion, appear relatively normal, suggesting that the small airways in these areas are less damaged. The segmental arteries are not larger than the adjacent bronchi and the pulmonary arteries are not engorged in the areas of hyperperfusion, as would be expected in cases of pulmonary hypertension (Fig 6a). **(b)** Mosaic attenuation in a 42-year-old woman with organizing pneumonia. Axial CT image of the lungs shows diffuse ground-glass opacity, creating mosaic attenuation. Note that the mildly dilated airways (arrows) extend into the higher-attenuation lung, while the airways in the normal lower-attenuation lung are normal in caliber. The distribution of the abnormal airways is the opposite of what is seen in many small airways diseases and can help differentiate between the causes.

Figure 8. Pulmonary edema in a 66-year-old woman who presented to the emergency department with acute shortness of breath. Coronal reformatted image from CT pulmonary angiography shows diffuse ground-glass opacity, with lobular areas of variable attenuation creating a mosaic pattern. Peribronchial cuffing (white arrow) due to edema can be easily confused with bronchial inflammation. However, although the bronchi are thickened, they are not distorted, there are no areas of endobronchial mucus plugging, and the thickening is most pronounced in the higher-attenuation areas of the lung, which all argue against a small airways cause. In addition, the pulmonary vasculature is not attenuated in the more lucent lung, which suggests a parenchymal cause, and the presence of ground-glass opacity, septal thickening (black arrows), and pleural effusions (not shown) makes pulmonary edema the most likely diagnosis.

the presence of centrilobular nodules on CT in conjunction with mosaic attenuation is a good clue that injury to the small airways is the cause of the mosaicism. In most instances, centrilobular or tree-in-bud nodules are a focal finding and commonly due to an infectious bronchiolitis. However, in certain diseases, hazy ill-defined centrilobular nodularity can itself create mosaic attenuation, especially when it is superimposed on diffuse ground-glass opacity. This is the case in hypersensitivity pneumonitis and in the spectrum of smoking-related lung diseases ranging from respiratory bronchiolitis to desquamative interstitial pneumonia.

In hypersensitivity pneumonitis, inflammation of the respiratory bronchioles occurs most commonly due to inhalation of an organic antigen, which creates both a type III and type IV hypersensitivity reaction (34,35). In the early stages of disease, airway-centered interstitial inflammation around the respiratory bronchioles (Fig 4c) leads to centrilobular nodules on imaging, whereas areas of organizing pneumonia can lead to varying degrees of ground-glass opacity on CT (36). Since the interstitial inflammation is airway centered, areas of hypoattenuated lung can be seen interspersed with the areas of ground-glass opacity and centrilobular nodularity, creating a pattern of diffuse lung disease where it can be difficult to localize any normal lung attenuation (Fig 10) (37). However, despite the often extensive degree of abnormality, the presence of upper lobe predominant centrilobular nodules, ground-glass opacity, and areas of hypoat-

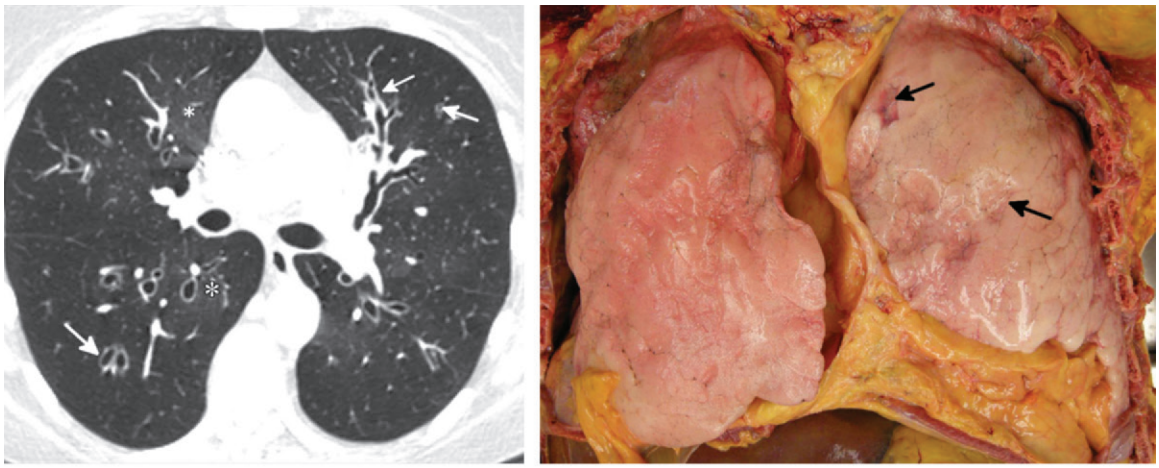

a. b.

Figure 9. Constrictive bronchiolitis in a 72-year-old woman with graft-versus-host disease. **(a)** Axial CT image shows a mosaic attenuation pattern, with predominantly hyperlucent lung with a few areas of normal lung attenuation (*). The bronchi are mildly bronchiectatic and are thickened (arrows). **(b)** Gross image of the lungs on autopsy shows that even after death and removal of the chest wall, the lungs remain inflated due to the severity of the constrictive bronchiolitis. Normally, the entire lung deflates after death. In this case, only a few secondary lobules deflate (arrows).

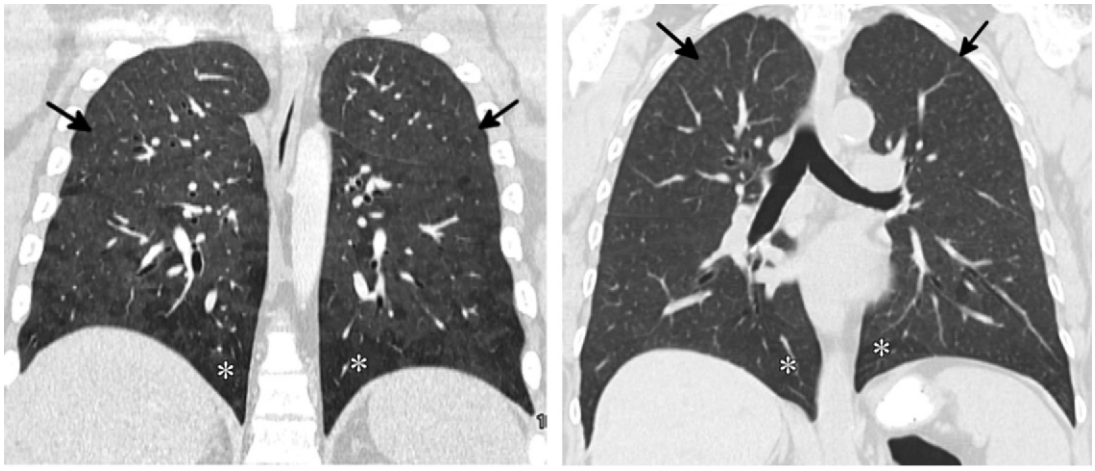

a. b.

Figure 10. Mosaic attenuation with ground-glass opacity and upper lobe predominant centrilobular nodules in two patients. **(a)** Coronal CT image in a 34-year-old man who has multiple parrots as pets shows relatively diffuse but upper lung predominant ground-glass opacity and centrilobular nodules (arrows) with areas of relative lobular hypoattenuation at the bases (*). Without expiration imaging, it is difficult to assess whether the areas of relative hypoattenuation are due to spared lung versus airtrapping. Open lung biopsy confirmed the diagnosis of hypersensitivity pneumonitis. **(b)** Coronal CT image in a 29-year-old man with worsening cough who smokes 1.5 packs of cigarettes a day shows hazy ground-glass opacity with upper lobe predominant centrilobular nodules (arrows) and some areas of relative hypoattenuation at the bases (*). Bronchoscopy confirmed the diagnosis of respiratory bronchiolitis. The appearance of respiratory bronchiolitis and nonfibrotic hypersensitivity pneumonitis can overlap, as both diseases initially lead to inflammation of the respiratory bronchioles. If emphysema is absent, a detailed clinical history is often needed to differentiate between the two diseases.

tenuation should suggest hypersensitivity pneumonitis as a possible cause. Early recognition of hypersensitivity pneumonitis improves the likelihood of proper treatment and disease regression, while continued exposure can lead to fibrotic disease (Fig 11), which is discussed in more detail later.

Respiratory bronchiolitis, respiratory bronchiolitis–interstitial lung disease, and desquamative interstitial pneumonia represent a spectrum of disease secondary to cigarette smoking in nearly all cases. In respiratory bronchiolitis, which can be an incidental finding in smokers at both imaging and histologic analysis, accumulations of macrophages with finely granular brown cytoplasmic pigment are present in the lumina of distal bronchioles, alveolar ducts, and adjacent alveoli. This is often associated with mild airway and interstitial inflammation, leading to ill-defined centrilobular nodules and mild ground-glass opacity (Fig 10). When a patient with

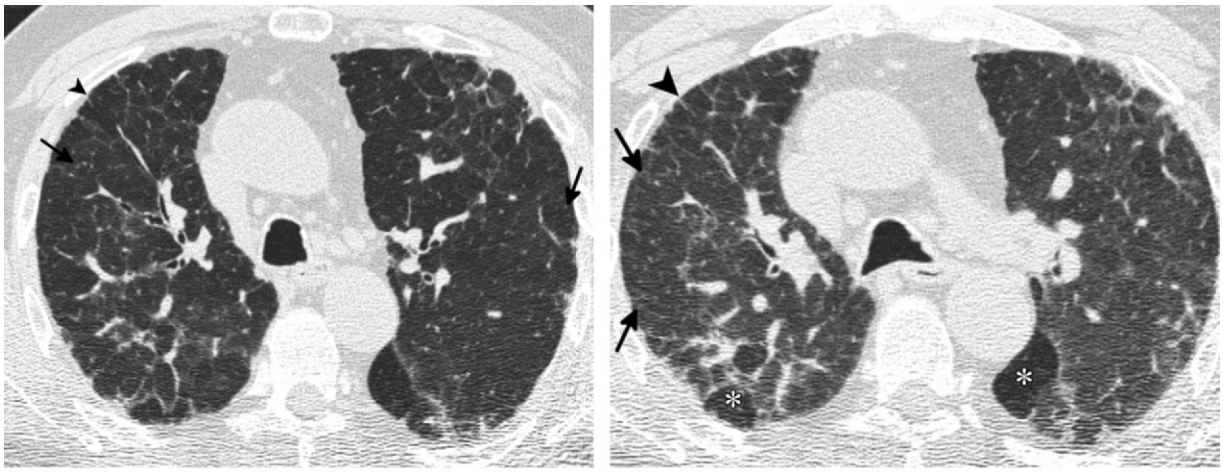

a. b.

Figure 11. Fibrotic hypersensitivity pneumonitis in a 61-year-old woman. **(a)** Axial CT image on inspiration shows mosaic attenuation with multiple varying areas of lung attenuation. Peripheral reticulation (arrowhead), due to fibrosis, was most severe in the mid and upper lung zones. A few centrilobular nodules can still be seen (arrows). **(b)** Axial CT image during expiration shows an increase in lung attenuation in most areas. A few areas of lung show no change in attenuation between the inspiration and expiration images, consistent with focal areas of airtrapping (*). The presence of mid and upper lung fibrosis with centrilobular nodules (arrows), reticulation (arrowhead), and areas of airtrapping place fibrotic hypersensitivity pneumonitis high in the differential diagnosis.

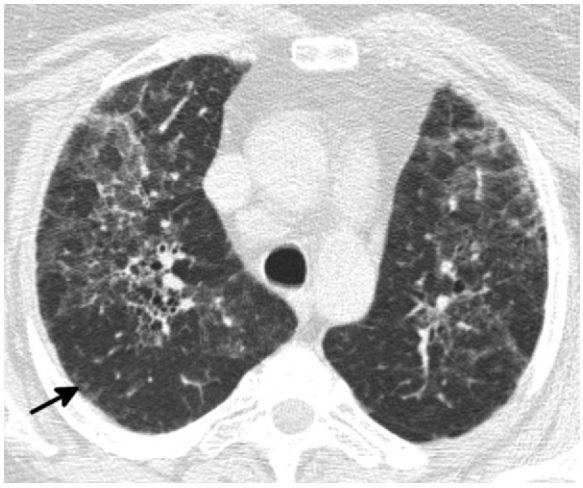

Figure 12. Desquamative interstitial pneumonia in a 50-year-old man who smokes two to three packs of cigarettes per day. Axial CT image of the upper lobes shows an atypical pattern of diffuse lung disease, with ground-glass opacity with a few areas of lobular sparing. In addition, ill-defined centrilobular nodules (arrow) due to coexistent respiratory bronchiolitis are present. This along with the history can help one make the diagnosis.

respiratory bronchiolitis becomes symptomatic and develops restrictive pulmonary function test abnormalities, a clinical diagnosis of respiratory bronchiolitis–interstitial lung disease is often made (38). Pathologically, the two are indistinguishable (39). Given that the bronchiolocentric site of disease is similar in both respiratory bronchiolitis and hypersensitivity pneumonitis, it is not surprising that the imaging features of the two can overlap, especially in the earlier stages of disease (40). Both often demonstrate upper lobe predominant centrilobular nodules and mosaic attenuation (37,38,41). One of the best methods of differentiating between the two relies on the presence of emphysema or a documented smoking history, as smoking can be protective against developing hypersensitivity pneumonitis due to immune modulation (40,42,43).

In desquamative interstitial pneumonia, airspace accumulations of macrophages with finely granular brown cytoplasmic pigment diffusely involve the alveoli of secondary lobules (38). This creates confluent areas of ground-glass opacity, which tend to be mid and lower lung zone predominant (44). Cystic change, which does not represent honeycombing, is often present and is most pronounced in areas of increased ground-glass opacity (45). In severe cases, fibrosis can lead to findings of reticulation and bronchiectasis. Due to the presence of coexistent respiratory bronchiolitis, the presence of upper lobe centrilobular nodules, if present, can help one make the diagnosis (Fig 12).

Assess the Pulmonary Vasculature

The size and morphology of the central and peripheral pulmonary arteries are helpful clues to differentiate vascular causes of mosaic attenuation from small airways disease and ground-glass opacity. The presence of enlarged pulmonary arteries should prompt evaluation for pulmonary hypertension as a cause of mosaic attenuation. Pulmonary arterial findings suggestive of pulmonary hypertension include central pulmonary artery enlargement, pulmonary artery–to-aorta

Figure 13. PAH in a 24-year-old woman with a mean pulmonary artery pressure of 64 mm Hg. **(a)** Axial image from CT pulmonary angiography (lung window) shows mosaic attenuation with more nodular areas of ground-glass opacity centered around the pulmonary arteries. This appearance is different than the more segmental areas of hyperattenuation and hypoattenuation seen in chronic thromboembolic disease. **(b)** Expiration CT image shows increased attenuation throughout the lung, excluding airtrapping and a small airways cause. **(c)** CT image shows transverse measurement of the main pulmonary artery, which is only 26 mm. However, the main pulmonary artery is larger than the aorta, which is abnormal. **(d)** Four-chamber CT image shows mild flattening of the interventricular septum (arrow) suggestive of increased right heart pressures, as the image was obtained during systole (atrioventricular valves are closed). There are also prominent trabeculae in the right ventricle (*), suggestive of right ventricular hypertrophy.

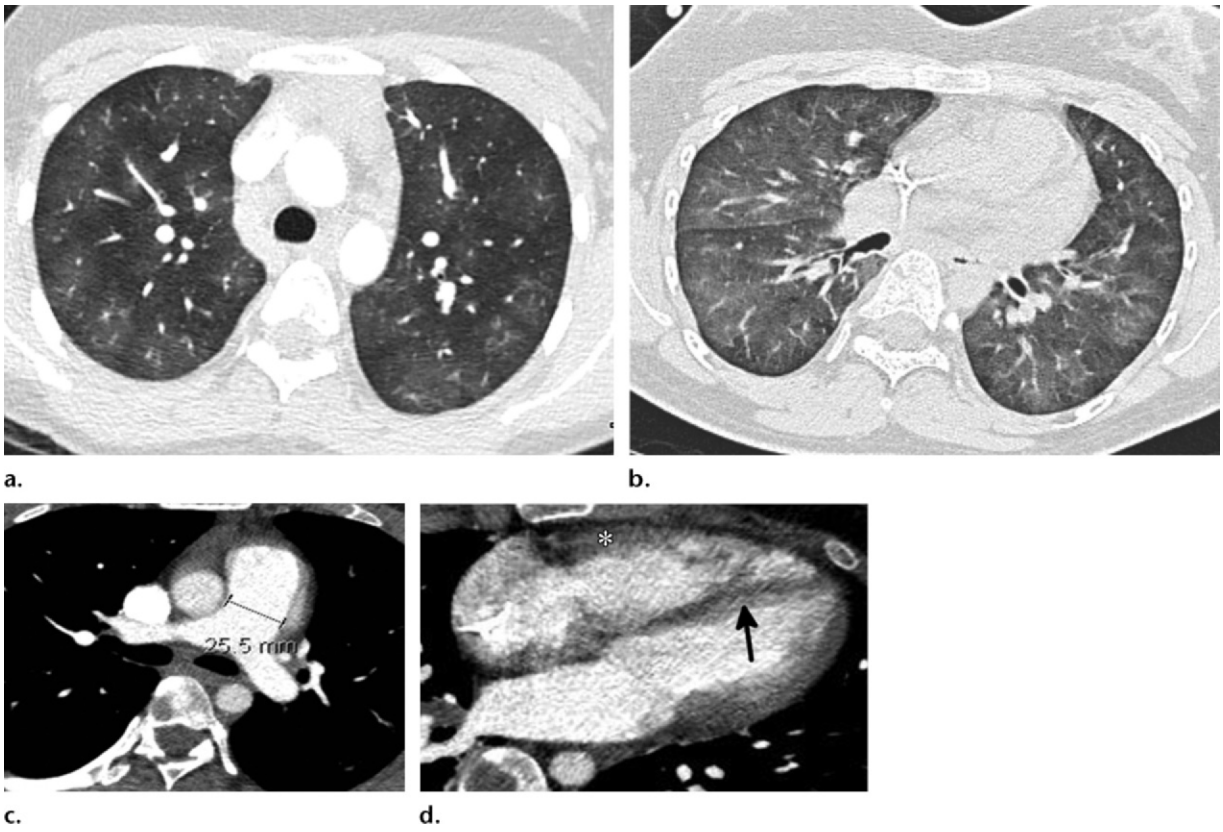

ratio greater than 1, and increased segmental artery-to-bronchus ratio.

Although the Framingham Heart Study set a normal cutoff value for pulmonary artery size at 29 mm for men and 27 mm for women (measured as the transverse diameter of the main pulmonary artery on an axial image at the level of the bifurcation of the right pulmonary artery), this isolated value is not specific for pulmonary hypertension, as multiple other factors can affect pulmonary artery size, including body mass index, systemic hypertension, diabetes, age, and underlying cardiovascular disease (46,47). A more accurate measurement is to compare the ratio of the diameter of the main pulmonary artery to that of the ascending aorta (transverse diameter measured on the same axial image as used for the main pulmonary artery measurement), where a ratio greater than 1 is suggestive of pulmonary hypertension (Fig 13) (48,49). In addition to the size of the main pulmonary artery, one should also assess the segmental artery-to-bronchus ratio. If this ratio is greater than 1 in three or more lobes, this finding is also highly specific for pulmonary hypertension (46).

In addition to assessing size of the pulmonary arteries, one should assess the morphology of the pulmonary vasculature. For instance, abruptly tapering or corkscrew vessels are associated with pulmonary hypertension, as are dilated bronchial or other systemic collaterals (50). In cases of CTEPH, which are important to recognize since invasive treatments are possible (51), close inspection of the pulmonary vasculature scans can demonstrate adherent thrombus (Fig 14), abrupt occlusion of pulmonary arteries, luminal irregularities with eccentric wall thickening, abrupt caliber change (often due to recanalization), and webs or bands (21,52,53).

Differentiating between PAH (also known as primary pulmonary hypertension) and CTEPH is not always easy. Classically, patients with mosaic attenuation due to CTEPH often demonstrate a well-demarcated segmental or subsegmental distribution of mosaicism due to the vascular distribution of thrombi, whereas the mosaic pattern in PAH often

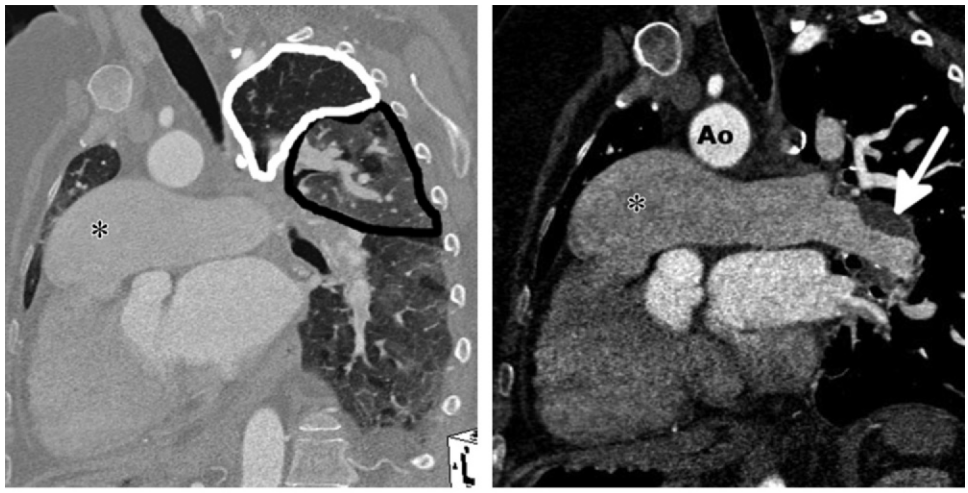

Figure 14. Mosaic attenuation in a 56-year-old man with chronic thromboembolic disease. **(a)** Sagittal CT image shows the difference in segmental pulmonary arterial size in areas of hypoattenuated lung due to vascular occlusion (white outline) versus in areas of hyperattenuated lung due to increased perfusion (black outline). The large airways are normal and the main pulmonary artery is enlarged (*). **(b)** Sagittal CT image (soft-tissue window) shows marked enlargement of the main pulmonary artery (*) compared with the aorta *(Ao)*. Chronic thrombus is present in the left pulmonary artery (arrow).

manifests as focal perivascular hyperattenuation or small scattered areas of low attenuation confined to the secondary pulmonary lobule (20). The perivascular areas of hyperattenuation may mimic discrete centrilobular ground-glass nodules that are of uncertain cause but thought to represent cholesterol granulomas, large plexogenic arterial lesions, or small systemic collateral arteries (Fig 13) (54). In addition, dilated peripheral arteries can have a corkscrew morphology (20). While adherent thrombus is a good clue to the presence of CTEPH, in situ thrombus and/or atherosclerosis may result from severe long-standing PAH and can sometimes be confused for CTEPH, so assessment of the pattern of mosaic attenuation is important for differentiation of these entities (20,55,56).

Look at the Heart

In the evaluation of pulmonary hypertension, CT provides not only an assessment of the lung parenchyma but also of the heart and pulmonary vasculature. Chronically elevated pulmonary pressures cause remodeling of the right heart, with right ventricular hypertrophy (free wall thickness > 4 mm), right ventricular dilatation (>1:1 ratio between right ventricular and left ventricular diameter on axial images), and spherical shape of the right ventricular chamber with straightening or leftward deviation of the interventricular septum (Figs 13, 15) (56). Right ventricular failure may manifest as dilatation of the inferior vena cava with reflux of contrast material into the hepatic veins (57). The presence of a dilated right heart (with or without hypertrophy) should always prompt a careful search for an undiagnosed cardiac shunt as the cause of pulmonary hypertension (Fig 15).

Whereas right ventricular hypertrophy in the setting of mosaic attenuation is associated with pulmonary hypertension, abnormalities of the left heart can point to other causes. In patients with left ventricular and/or left atrial dilatation, pulmonary edema may be the cause of the mosaic appearance, especially if interlobular septal thickening is present.

Assess for Interlobular Septal Thickening

Smooth interlobular septal thickening occurs when the lymphatics or veins in the secondary pulmonary lobule become dilated and the septum itself becomes edematous. The presence of diffuse ground-glass opacity with superimposed interlobular septal thickening is seen in only a few disease states and can help narrow the differential diagnosis of a mosaic pattern. Patient history can further help narrow the differential diagnosis.

Pulmonary edema occurs when there is disruption of the physiologic equilibrium between fluid transudation or exudation and lymphatic absorption (58). Causes of edema can be further divided into hydrostatic and nonhydrostatic. In hydrostatic pulmonary edema, hydrostatic pressure is raised due to left ventricular failure or fluid overload. Nonhydrostatic edema is caused by damage to the alveolar and vascular endothelium that results in fluid permeability (59). Ground-glass opacity occurs as fluid begins to fill the alveolar spaces (58). In addition to ground-glass opacities and interlobular septal

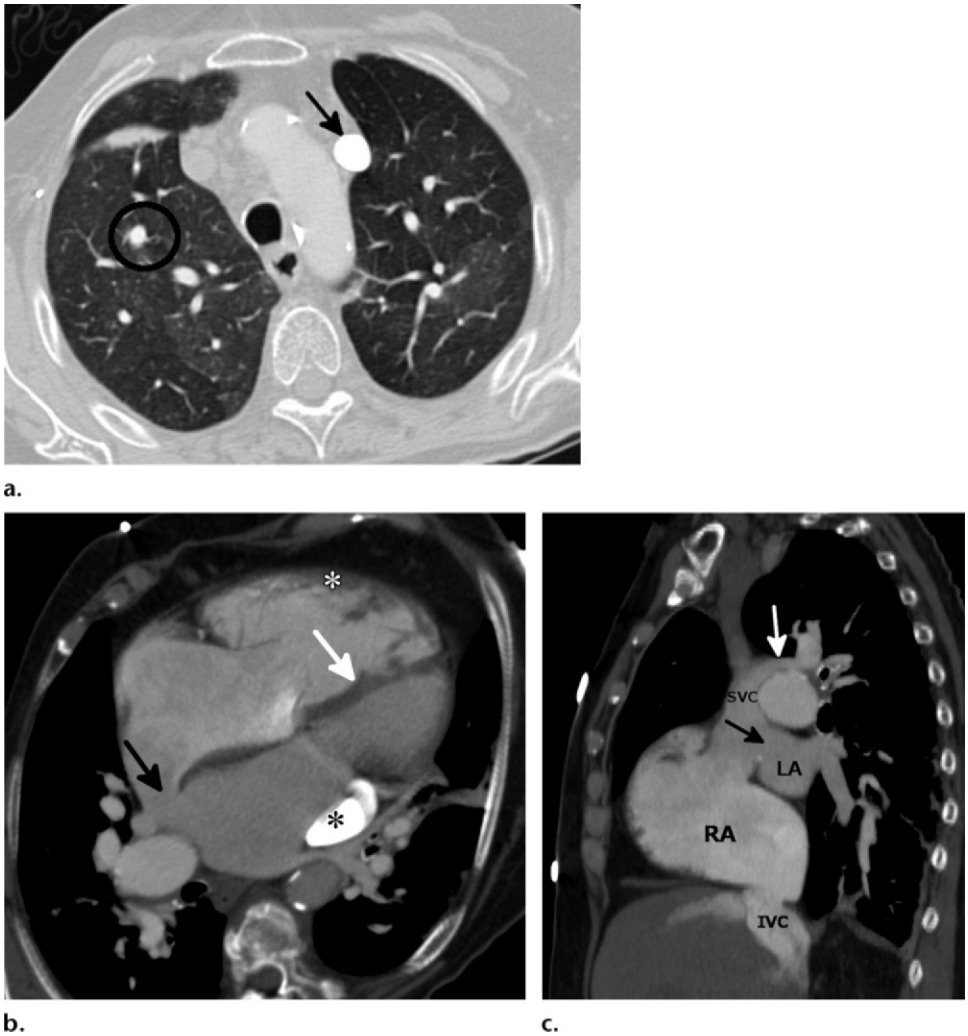

Figure 15. CT pulmonary angiography performed to assess for chronic thromboembolic disease in a 75-year-old woman with newly diagnosed pulmonary hypertension. **(a)** Axial CT image of the upper lobes shows prominent mosaic attenuation. A subsegmental right upper lobe artery is much larger than the associated subsegmental bronchus (circle). The airways are normal. A left superior vena cava (SVC) is present (arrow). **(b)** Four-chamber CT image shows enlargement of the right atrium and right ventricle, flattening of the interventricular septum (white arrow), and thickening of the anterior wall of the right ventricle (white *). A previously undiagnosed sinus venosus atrial septal defect is present (black arrow). The left SVC (black *) is dilated. **(c)** Sagittal CT image shows the right upper lobe pulmonary vein (white arrow) draining into the right SVC, consistent with partial anomalous pulmonary venous return. This is a common finding associated with a sinus venosus atrial septal defect (black arrow), which allows direct communication between the right atrium *(RA)* and partially visualized left atrium *(LA)*. The right atrium is dilated and there is reflux of contrast material into the dilated inferior vena cava *(IVC)* due to elevated right heart pressures. It is important to assess the heart in the presence of mosaic attenuation, as it can provide clues to the underlying cause.

thickening, other CT findings of hydrostatic pulmonary edema that can help differentiate it from other causes include peribronchial thickening and pleural effusions (Fig 8). An enlarged heart size is another clue to increased fluid status in hydrostatic pulmonary edema. A gravitational anteroposterior gradient is often observed in a recumbent patient.

P jirovecii pneumonia should be suspected in patients with acquired immunodeficiency syndrome (AIDS) with a CD4+ level of less than 200 cells per cubic millimeter or in other immunosuppressed patients who present with diffuse but perihilar or upper lobe predominant ground-glass opacities and septal thickening at CT (Fig 16) (60). Sparing of the lung periphery is a common finding, thought to be due to the bucket-handle motion of the rib cage during respiration, which enhances lymphatic drainage.

In the acute stages of diffuse alveolar hemorrhage, red blood cells can fill or partially fill the alveoli, leading to areas of consolidation and ground-glass opacity, respectively (61). Although the hemorrhage can be focal or widespread, the

accumulation of hemosiderin-laden macrophages in alveoli may give a nodular appearance to the ground-glass opacity at CT (62,63). As the hemorrhage starts to clear, interlobular septal thickening begins to occur and is seen in up to two-thirds of patients with diffuse alveolar hemorrhage (Fig 6c) (64). Interlobular septal thickening also tends to be more prominent in patients with recurrent hemorrhage (61). If the bleeding stops, the hemorrhage can clear in a matter of days. Numerous causes of diffuse alveolar hemorrhage exist, including vasculitis (granulomatosis with polyangiitis, Churg-Strauss syndrome), autoimmune disease (eg, antiphospholipid syndrome, Goodpasture syndrome), hypercoagulable states, infection, renal failure, and drugs (eg, cocaine, amiodarone) (65,66). Therefore, patient history can be helpful in making the diagnosis. Hemoptysis is present in only about one-third of patients, as the lung can absorb a large amount of blood before the extension of hemorrhage into the larger airways (67).

Interlobular septal thickening with a mosaic pattern can also occur in both diffuse alveolar damage and organizing pneumonia, as focal areas of spared normal-attenuation secondary lobules are adjacent to involved lung (Fig 17) (30). These areas of normal lung interspersed in areas of extensive parenchymal abnormality occur due to the zonal nature of the injury to the alveolar epithelium, which is mirrored at pathologic analysis (68). Perilobular opacities, which are often subpleural, are a common finding in organizing pneumonia and are often seen in up to 57% of patients (69,70). They appear as poorly defined curvilinear or polygonal opacities that border the secondary pulmonary lobule and may represent a combination of dilated septal lymphatics and septal fibrosis.

Unusual causes of septal thickening include PVOD and PCH, which also result in pulmonary hypertension from fibrous obliteration of the postcapillary venules and proliferation of capillary channels within alveolar walls, respectively (71). Although initially thought to represent two disorders, pathologic data suggest that these two entities represent a varied expression of a single disorder (72). These entities are often misdiagnosed as primary PAH; however, distinction is critical as standard vasodilator therapy may induce fatal pulmonary edema in these patients (73). While definitive diagnosis requires biopsy, imaging plays an important role in evaluation of suspected PVOD and PCH.

Prominent smooth interlobular septal thickening is a characteristic finding in PVOD. Variable amounts of ground-glass opacity and oligemia can create mosaic attenuation, which can be seen in one-half of patients (71,74). In patients with PCH, ill-defined centrilobular nodules predominate. However, the imaging and pathologic findings of PVOD and PCH are often seen in the same patient (Fig 18) (71,72). Pleural effusions are also a common finding, but the left heart and pulmonary veins are normal in size. This constellation of findings superimposed on findings of pulmonary hypertension including dilated central pulmonary arteries, right ventricular hypertrophy, and flattening of the interventricular septum can help one make the diagnosis.

Figure 16. Mosaic attenuation in a 43-year-old man with AIDS, a CD4 count of 23 cells per cubic millimeter, and worsening shortness of breath and cough. Axial CT image shows diffuse ground-glass opacity with scattered areas of lobular sparing, creating mosaic attenuation. Areas of septal thickening are present (arrow), which narrows the differential diagnosis, which includes edema, hemorrhage, and certain infections. Given the patient's history, *P jirovecii* pneumonia was suspected and confirmed with bronchoscopy.

Figure 17. Mosaic attenuation and septal thickening in diffuse alveolar damage in a 26-year-old patient with acute respiratory distress syndrome. Axial CT image of the lower lobes shows a geographic distribution of consolidation and ground-glass opacity. There is clear demarcation between involved lung (*) and spared lobules (arrowhead), which creates mosaic attenuation.

Look for Signs of Fibrosis

Signs of fibrosis on high-resolution CT favor an interstitial process as the cause of the mosaicism.

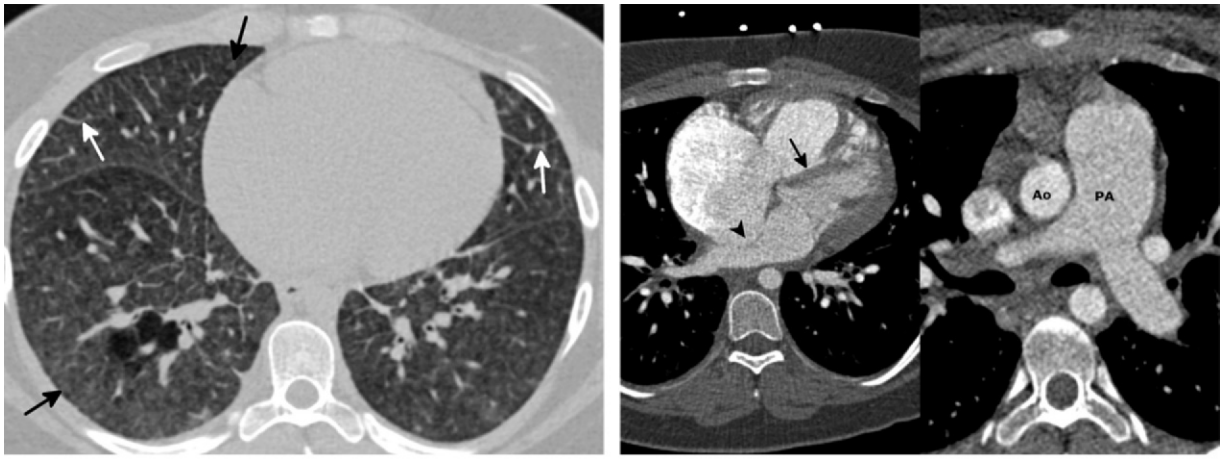

a. b.

Figure 18. PVOD and PCH in a 36-year-old woman diagnosed as having PAH. **(a)** Axial CT image shows varying degrees of ground-glass opacity with areas of septal thickening (white arrows) and ill-defined centrilobular nodules (black arrows), creating mosaic attenuation. **(b)** Axial CT images at the level of the heart (left) and pulmonary artery *(PA)* (right) show marked flattening of the interventricular septum (arrow) and right ventricular hypertrophy due to severe pulmonary hypertension. Bulging of the interatrial septum toward the left atrium (arrowhead) is due to significantly elevated right atrial pressures. The pulmonary artery is enlarged with a diameter greater than that of the aorta *(Ao)*.

Whereas the acute phase of diffuse alveolar damage can demonstrate patchy ground-glass opacities with interlobular septal thickening, the organizing phase of diffuse alveolar damage typically shows findings of fibrosis such as reticulation, bronchiectasis, and volume loss (30). The fibrosis seen in organizing pneumonia is well depicted on CT and is often demonstrated as areas of peribronchiolar ground-glass opacity or perilobular thickening with traction bronchiectasis and reticulation in areas of injured lung. These areas of fibrosis may be most conspicuous after resolution of the consolidation. In some instances, the residual fibrosis is lower lobe predominant, peribronchiolar in distribution, and demonstrates subpleural sparing, findings commonly associated with nonspecific interstitial pneumonia (75,76). Bronchiectasis will be most pronounced in these areas of fibrosis, which demonstrate increased ground-glass opacity due to the interstitial abnormality.

Although many patterns of fibrotic hypersensitivity pneumonitis have been described, in most instances patients present with mid and upper lung predominant fibrosis. Mosaic attenuation is commonly present and can help in differentiation from other causes of pulmonary fibrosis (77). In addition, since antigenic exposure often continues, signs of bronchiolar inflammation, namely centrilobular nodules, are often present and can again help differentiate fibrotic hypersensitivity pneumonitis from other disease processes (Fig 11). Although fibrosis is not common in small airways or vascular causes of mosaic attenuation, peripheral areas of scarring from prior infarct can be seen in patients with CTEPH.

Look for Additional Clues Inside or Outside the Thorax

Although small airway injury can on occasion be idiopathic, most cases of inflammatory or constrictive bronchiolitis have known causes. Some include systemic diseases that can lead to imaging findings outside the lung parenchyma, which can help one make the correct diagnosis. For instance, among the connective tissue diseases, rheumatoid arthritis is the most likely to cause constrictive bronchiolitis, and lung disease may be the initial presenting manifestation in 10%–20% of patients (78,79). Therefore, close inspection of the joint spaces at chest CT, most notably the shoulders, can provide clues to the underlying cause of the mosaic attenuation and potentially help one make the initial diagnosis of a systemic disease (Fig 19).

In those who have undergone lung transplantation, constrictive bronchiolitis is the clinicopathologic finding in chronic rejection. Unfortunately, it is a common complication and occurs in at least 50% of transplant recipients at 5 years (80). Therefore, the presence of clamshell median sternotomy wires, which are commonly used in bilateral lung transplantation, in a patient with mosaic attenuation is a good hint as to the underlying cause (Fig 5).

In patients with mosaic attenuation and scattered small rounded parenchymal nodules, one may think of DIPNECH (Fig 20). This condition is most commonly seen in middle-aged nonsmoking women and is sometimes misdiagnosed as adult-onset asthma (81,82). DIPNECH is a primary proliferation of pulmonary neuroendocrine

cells that involves both the terminal and respiratory bronchioles and can lead to constrictive bronchiolitis and mosaic attenuation on CT (83). When these proliferations of neuroendocrine cells become large enough, they can be visualized on CT as discrete pulmonary nodules, which are classified as carcinoid tumorlets if less than 5 mm in diameter and as carcinoid tumors if 5 mm or greater in diameter. Although not always visible, if multiple rounded nodules are present in the setting of mosaic attenuation in a middle-aged woman, one should raise the possibility of DIPNECH (82,83).

The presence of parenchymal cysts in the setting of ground-glass opacity can help differentiate *Pneumocystis* pneumonia from other causes of ground-glass opacity and interlobular septal thickening. However, this finding occurs in only as much as one-third of patients (84). Superimposed dense consolidation can also help in differentiation but can also be seen with diffuse alveolar hemorrhage.

Perform Expiratory Imaging

One of the best ways to distinguish small airways disease from other forms of mosaic attenuation is by demonstration of airtrapping at expiratory imaging (Fig 1). At expiratory CT in patients with non–airways-related causes of mosaic attenuation, the lungs should show a diffuse increase in attenuation. In cases of PAH, one will usually see a diffuse increase in attenuation in both the abnormal lucent lung and the normal higher-attenuation lung (Fig 13) (11). Similarly, in cases of diffuse ground-glass opacity leading to mosaic attenuation, one should see increased attenuation in both the normal more lucent lung and the abnormal higher-attenuation lung (Fig 2).

There are various techniques for expiratory imaging, but it is usually performed with thin-collimation axial scans performed at two to six levels throughout the lungs at forced expiration, which are reconstructed with a high spatial resolution algorithm (85). Although institutional variations exist, common indications that may prompt the addition of expiratory imaging to a CT scan (if not already ordered by the referring clinical) include worsening symptoms in any patient with a known bronchiolar disorder (Table 1) or in a patient with a risk factor for constrictive bronchiolitis (Table 2). However, the finding of mosaic attenuation may be an incidental finding without a clear cause, and in these instances the patient may benefit from returning to the radiology department for dedicated expiration imaging if it can help in diagnosis.

The presence of airtrapping is an excellent clue to the diagnosis of small airways disease, but there are a few pitfalls that should be avoided.

a.

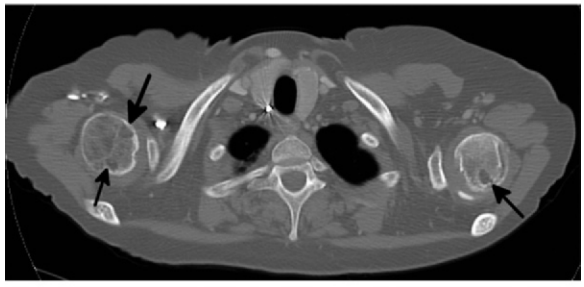

b.

Figure 19. Mosaic attenuation in a 41-year-old woman with shortness of breath. **(a)** Axial CT image shows prominent mosaic attenuation with well-defined borders between areas of differing attenuation. Expiratory imaging was not performed, which precluded diagnosis of airtrapping. **(b)** Axial CT image at the level of the shoulders (bone window) shows multiple erosions in the humeral heads (arrows). Review of the patient's electronic medical record confirmed the diagnosis of rheumatoid arthritis. A presumptive diagnosis of constrictive bronchiolitis due to rheumatoid arthritis was made on the basis of the imaging findings and later confirmed at biopsy.

First, as discussed earlier, areas of airtrapping can be seen in normal patients and some degree of heterogeneity of the lung parenchyma is expected at expiratory imaging (Fig 3) (8,86). Second, although expiratory imaging sequences may be ordered, they may not be adequately performed. This can be due to lack of patient effort or poor coaching from a technologist.

Therefore, it is imperative that the membranous (posterior) wall of the trachea and posterior wall of the main-stem bronchi are assessed in each patient undergoing expiratory imaging. With good expiratory effort, the posterior wall of these structures should bow inward due to increased intrathoracic pressure (Fig 1). On the other hand, patients who are unable to follow breathing instruction may breathe during an inspiratory CT scan, leading to its acquisition during the expiratory phase. Again, it is important to inspect the posterior wall of the trachea on all CT scans of the chest so one can prevent diagnosing the nor-

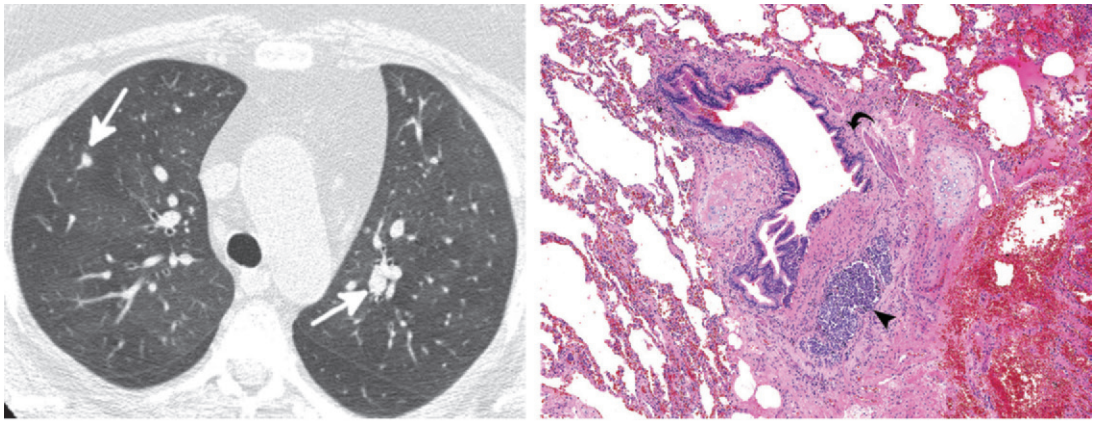

a. b.

Figure 20. DIPNECH in a 48-year-old woman diagnosed with adult-onset asthma. **(a)** Axial CT image of the mid lung zone shows mosaic attenuation with small pulmonary nodules ranging in size from 3 to 6 mm (arrows). **(b)** Photomicrograph from a patient with DIPNECH shows a small bronchus with a carcinoid tumorlet (arrowhead) associated with airway fibrosis (arrow). (Original magnification, ×60; H-E stain.)

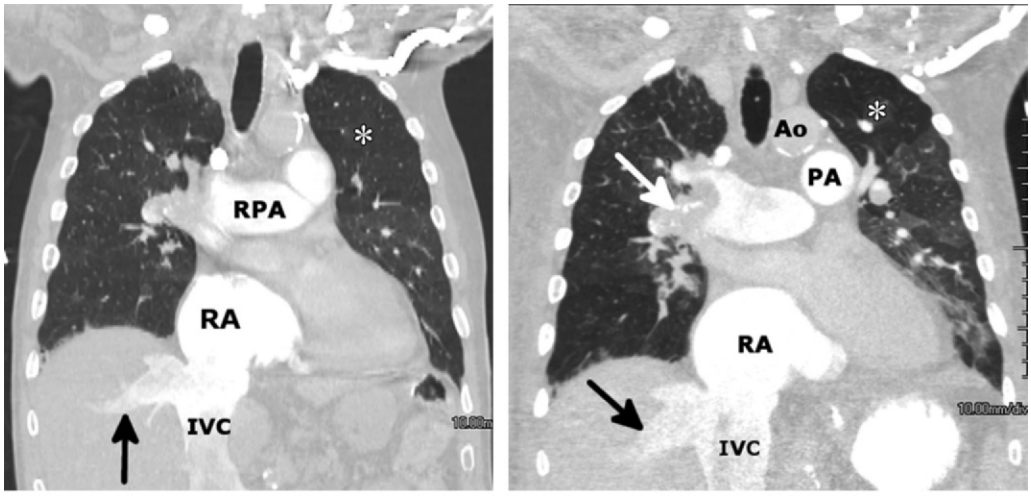

a. b.

Figure 21. Airtrapping in a 66-year-old man with chronic thromboembolic disease (CTEPH). **(a)** Coronal CT image from an initial scan performed during inspiration shows mosaic attenuation with areas of decreased attenuation (*), as well as dilatation of the right pulmonary artery *(RPA)*, right atrium *(RA)*, and inferior vena cava *(IVC)*, consistent with increased right atrial pressures. There is reflux of contrast material into the hepatic veins (arrow). **(b)** Coronal CT image from a scan performed 2 days later during expiration again shows the areas of airtrapping (*). Airtrapping can occasionally be seen in patients with CTEPH. However, this is just one finding, while there are numerous additional findings that help one make the diagnosis of chronic thromboembolic disease, such as diameter of the main pulmonary artery *(PA)* larger than that of the aorta *(Ao)*, dilated right atrium *(RA)*, reflux of contrast material into the dilated inferior vena cava *(IVC)* and hepatic veins (black arrow), and presence of adherent calcified thrombus in the right pulmonary artery (white arrow).

mal increased lung attenuation during expiration as abnormal parenchymal ground-glass opacity.

In addition, the presence of airtrapping can, on occasion, be seen in patients with pulmonary hypertension or infiltrative diseases. For instance, the presence of airtrapping has been reported in patients with chronic thromboembolic disease due to reactive bronchoconstriction (Fig 21). Certain causes of ground-glass opacity leading to mosaic attenuation, namely hypersensitivity pneumonitis, will demonstrate airtrapping on expiration since the mechanism of disease primarily involves the respiratory bronchioles (Fig 11). Similarly, in cases of desquamative interstitial pneumonia, coexistent respiratory bronchiolitis can lead to airtrapping on expiration.

Lastly, mixed diseases can occur. Patients with airtrapping due to small airways disease may also have small vessel disease or causes of ground-glass opacity (Fig 22). Therefore, the presence of airtrapping is just one finding and should be used in conjunction with other imaging findings such

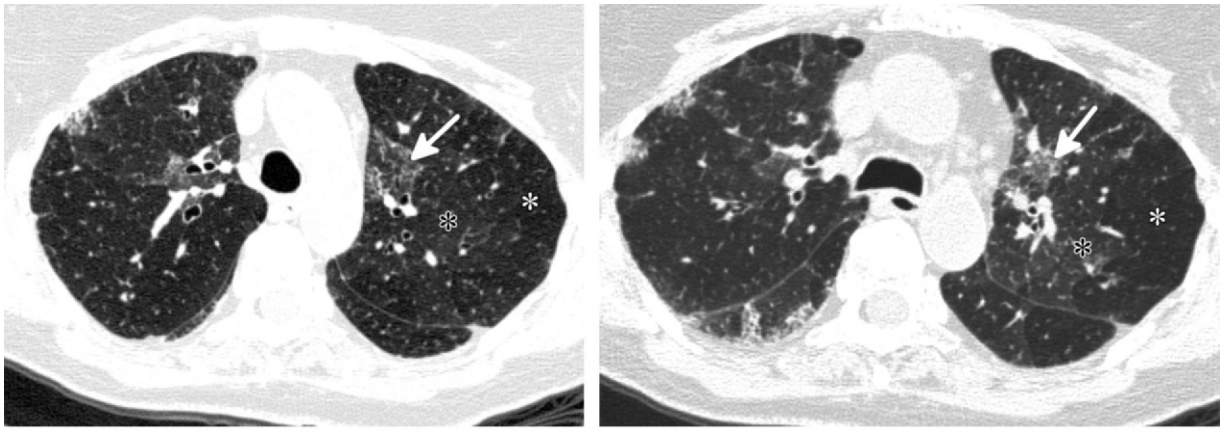

a. b.

Figure 22. Inspiratory and expiratory imaging in a 60-year-old woman with rheumatoid arthritis. **(a)** Inspiratory CT image shows relative areas of decreased attenuation (white ∗) adjacent to areas of relative increased attenuation (black ∗). Scattered areas of ground-glass opacity are present (arrow). **(b)** CT image at the same level during expiration shows that multiple areas of relative higher attenuation have increased in attenuation (black ∗), which excludes airtrapping and suggests that this lung is relatively normal. Areas of decreased attenuation at inspiratory imaging have not changed in attenuation due to airtrapping (white ∗). Areas of ground-glass opacity have also increased in attenuation (arrow), confirming the absence of airtrapping in these regions. Subsequent open-lung biopsy confirmed the presence of constrictive bronchiolitis, corresponding to the areas of airtrapping, and of organizing pneumonia, corresponding to the areas of ground-glass opacity. Both these disease processes can occur in patients with rheumatoid arthritis.

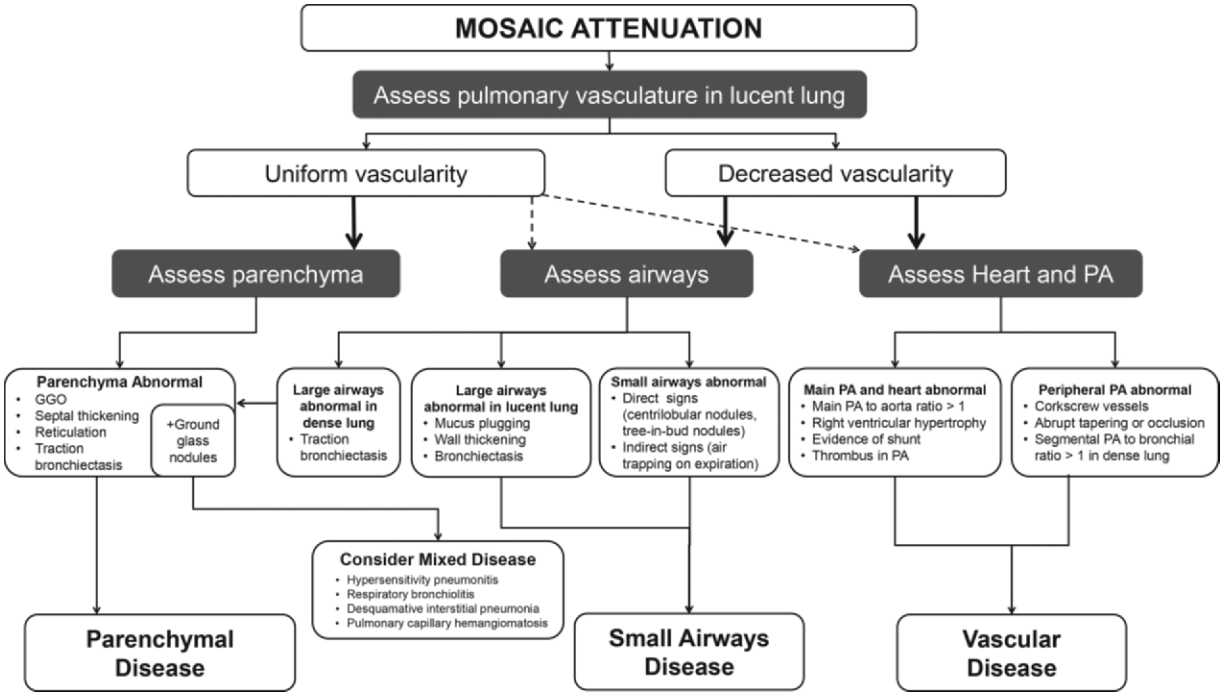

Figure 23. Flowchart for diagnosis of mosaic attenuation. Although uniform vascularity suggests a parenchymal cause of mosaic attenuation, make sure to still check the airways, pulmonary arteries, and heart (dashed lines), as a decrease in vascularity may be difficult to perceive in mixed or early disease states. *GGO* = ground-glass opacity, *PA* = pulmonary artery.

as bronchial and pulmonary artery morphology to make a final diagnosis.

Conclusion

Mosaic attenuation is a common finding among a wide range of causes that can involve the airways, pulmonary vasculature, alveoli, and interstitium. Although differentiation can be difficult, the differential diagnosis can be narrowed by recognizing various imaging manifestations (Fig 23), which can help guide management.

References

1. Ryu JH, Myers JL, Swensen SJ. Bronchiolar disorders. Am J Respir Crit Care Med 2003;168(11):1277–1292.
2. Arakawa H, Webb WR, McCowin M, Katsou G, Lee KN, Seitz RF. Inhomogeneous lung attenuation at thin-

section CT: diagnostic value of expiratory scans. Radiology 1998;206(1):89–94.
3. Worthy SA, Müller NL, Hartman TE, Swensen SJ, Padley SP, Hansell DM. Mosaic attenuation pattern on thin-section CT scans of the lung: differentiation among infiltrative lung, airway, and vascular diseases as a cause. Radiology 1997;205(2):465–470.
4. Webb WR, Stern EJ, Kanth N, Gamsu G. Dynamic pulmonary CT: findings in healthy adult men. Radiology 1993;186(1):117–124.
5. Park CS, Müller NL, Worthy SA, Kim JS, Awadh N, Fitzgerald M. Airway obstruction in asthmatic and healthy individuals: inspiratory and expiratory thin-section CT findings. Radiology 1997;203(2):361–367.
6. Verschakelen JA, Van fraeyenhoven L, Laureys G, Demedts M, Baert AL. Differences in CT density between dependent and nondependent portions of the lung: influence of lung volume. AJR Am J Roentgenol 1993;161(4):713–717.
7. Wittram C, Batt J, Rappaport DC, Hutcheon MA. Inspiratory and expiratory helical CT of normal adults: comparison of thin section scans and minimum intensity projection images. J Thorac Imaging 2002;17(1):47–52.
8. Mets OM, van Hulst RA, Jacobs C, van Ginneken B, de Jong PA. Normal range of emphysema and air trapping on CT in young men. AJR Am J Roentgenol 2012;199(2):336–340.
9. Lee KW, Chung SY, Yang I, Lee Y, Ko EY, Park MJ. Correlation of aging and smoking with air trapping at thin-section CT of the lung in asymptomatic subjects. Radiology 2000;214(3):831–836.
10. Pipavath SJ, Lynch DA, Cool C, Brown KK, Newell JD. Radiologic and pathologic features of bronchiolitis. AJR Am J Roentgenol 2005;185(2):354–363.
11. Stern EJ, Swensen SJ, Hartman TE, Frank MS. CT mosaic pattern of lung attenuation: distinguishing different causes. AJR Am J Roentgenol 1995;165(4):813–816.
12. Burgel PR, Bergeron A, de Blic J, et al. Small airways diseases, excluding asthma and COPD: an overview. Eur Respir Rev 2013;22(128):131–147.
13. Webb WR. Thin-section CT of the secondary pulmonary lobule: anatomy and the image—the 2004 Fleischner lecture. Radiology 2006;239(2):322–338.
14. Howling SJ, Hansell DM, Wells AU, Nicholson AG, Flint JD, Müller NL. Follicular bronchiolitis: thin-section CT and histologic findings. Radiology 1999;212(3):637–642.
15. Corren J. Small airways disease in asthma. Curr Allergy Asthma Rep 2008;8(6):533–539.
16. Churg A, Wright JL, Wiggs B, Paré PD, Lazar N. Small airways disease and mineral dust exposure: prevalence, structure, and function. Am Rev Respir Dis 1985;131(1):139–143.
17. Poletti V, Casoni G, Chilosi M, Zompatori M. Diffuse panbronchiolitis. Eur Respir J 2006;28(4):862–871.
18. Visscher DW, Myers JL. Bronchiolitis: the pathologist's perspective. Proc Am Thorac Soc 2006;3(1):41–47.
19. Hansell DM. Small airways diseases: detection and insights with computed tomography. Eur Respir J 2001;17(6):1294–1313.
20. Grosse C, Grosse A. CT findings in diseases associated with pulmonary hypertension: a current review. RadioGraphics 2010;30(7):1753–1777.
21. Sherrick AD, Swensen SJ, Hartman TE. Mosaic pattern of lung attenuation on CT scans: frequency among patients with pulmonary artery hypertension of different causes. AJR Am J Roentgenol 1997;169(1):79–82.
22. Chung MP, Yi CA, Lee HY, Han J, Lee KS. Imaging of pulmonary vasculitis. Radiology 2010;255(2):322–341.
23. Hansell DM, Bankier AA, MacMahon H, McLoud TC, Müller NL, Remy J. Fleischner Society: glossary of terms for thoracic imaging. Radiology 2008;246(3):697–722.
24. Gotway MB, Reddy GP, Webb WR, Elicker BM, Leung JW. High-resolution CT of the lung: patterns of disease and differential diagnoses. Radiol Clin North Am 2005;43(3):513–542, viii.
25. Delaunois L. Anatomy and physiology of collateral respiratory pathways. Eur Respir J 1989;2(9):893–904.
26. Task Force for Diagnosis and Treatment of Pulmonary Hypertension of European Society of Cardiology (ESC); European Respiratory Society (ERS); International Society of Heart and Lung Transplantation (ISHLT), et al. Guidelines for the diagnosis and treatment of pulmonary hypertension. Eur Respir J 2009;34(6):1219–1263.
27. Engeler CE, Tashjian JH, Trenkner SW, Walsh JW. Ground-glass opacity of the lung parenchyma: a guide to analysis with high-resolution CT. AJR Am J Roentgenol 1993;160(2):249–251.
28. Remy-Jardin M, Remy J, Giraud F, Wattinne L, Gosselin B. Computed tomography assessment of ground-glass opacity: semiology and significance. J Thorac Imaging 1993;8(4):249–264.
29. Remy-Jardin M, Giraud F, Remy J, Copin MC, Gosselin B, Duhamel A. Importance of ground-glass attenuation in chronic diffuse infiltrative lung disease: pathologic-CT correlation. Radiology 1993;189(3):693–698.
30. Kligerman SJ, Franks TJ, Galvin JR. Organization and fibrosis as a response to lung injury in diffuse alveolar damage, organizing pneumonia, and acute fibrinous and organizing pneumonia. RadioGraphics 2013;33(7):1951–1975.
31. Schwickert HC, Schweden F, Schild HH, et al. Pulmonary arteries and lung parenchyma in chronic pulmonary embolism: preoperative and postoperative CT findings. Radiology 1994;191(2):351–357.
32. Bergin CJ, Rios G, King MA, Belezzuoli E, Luna J, Auger WR. Accuracy of high-resolution CT in identifying chronic pulmonary thromboembolic disease. AJR Am J Roentgenol 1996;166(6):1371–1377.
33. Don C, Johnson R. The nature and significance of peribronchial cuffing in pulmonary edema. Radiology 1977;125(3):577–582.
34. Mohr LC. Hypersensitivity pneumonitis. Curr Opin Pulm Med 2004;10(5):401–411.
35. Bourke SJ, Dalphin JC, Boyd G, McSharry C, Baldwin CI, Calvert JE. Hypersensitivity pneumonitis: current concepts. Eur Respir J Suppl 2001;32:81s–92s.
36. Takemura T, Akashi T, Ohtani Y, Inase N, Yoshizawa Y. Pathology of hypersensitivity pneumonitis. Curr Opin Pulm Med 2008;14(5):440–454.
37. Silva CI, Churg A, Müller NL. Hypersensitivity pneumonitis: spectrum of high-resolution CT and pathologic findings. AJR Am J Roentgenol 2007;188(2):334–344.
38. Heyneman LE, Ward S, Lynch DA, Remy-Jardin M, Johkoh T, Müller NL. Respiratory bronchiolitis, respiratory bronchiolitis-associated interstitial lung disease, and desquamative interstitial pneumonia: different entities or part of the spectrum of the same disease process? AJR Am J Roentgenol 1999;173(6):1617–1622.
39. Fraig M, Shreesha U, Savici D, Katzenstein AL. Respiratory bronchiolitis: a clinicopathologic study in current smokers, ex-smokers, and never-smokers. Am J Surg Pathol 2002;26(5):647–653.
40. Lynch DA, Newell JD, Logan PM, King TE Jr, Müller NL. Can CT distinguish hypersensitivity pneumonitis from idiopathic pulmonary fibrosis? AJR Am J Roentgenol 1995;165(4):807–811.
41. Attili AK, Kazerooni EA, Gross BH, Flaherty KR, Myers JL, Martinez FJ. Smoking-related interstitial lung disease: radiologic-clinical-pathologic correlation. RadioGraphics 2008;28(5):1383–1396; discussion 1396–1398.
42. Vassallo R, Tamada K, Lau JS, Kroening PR, Chen L. Cigarette smoke extract suppresses human dendritic cell function leading to preferential induction of Th-2 priming. J Immunol 2005;175(4):2684–2691.
43. Israël-Assayag E, Dakhama A, Lavigne S, Laviolette M, Cormier Y. Expression of costimulatory molecules on alveolar macrophages in hypersensitivity pneumonitis. Am J Respir Crit Care Med 1999;159(6):1830–1834.
44. Hartman TE, Primack SL, Swensen SJ, Hansell D, McGuinness G, Müller NL. Desquamative interstitial pneumonia: thin-section CT findings in 22 patients. Radiology 1993;187(3):787–790.
45. Koyama M, Johkoh T, Honda O, et al. Chronic cystic lung disease: diagnostic accuracy of high-resolution CT in 92 patients. AJR Am J Roentgenol 2003;180(3):827–835.
46. Tan RT, Kuzo R, Goodman LR, Siegel R, Haasler GB, Presberg KW. Utility of CT scan evaluation for predicting pulmonary hypertension in patients with parenchymal lung

disease. Medical College of Wisconsin Lung Transplant Group. Chest 1998;113(5):1250–1256.
47. Truong QA, Massaro JM, Rogers IS, et al. Reference values for normal pulmonary artery dimensions by noncontrast cardiac computed tomography: the Framingham Heart Study. Circ Cardiovasc Imaging 2012;5(1):147–154.
48. Ng CS, Wells AU, Padley SP. A CT sign of chronic pulmonary arterial hypertension: the ratio of main pulmonary artery to aortic diameter. J Thorac Imaging 1999;14(4):270–278.
49. Devaraj A, Wells AU, Meister MG, Corte TJ, Wort SJ, Hansell DM. Detection of pulmonary hypertension with multidetector CT and echocardiography alone and in combination. Radiology 2010;254(2):609–616.
50. Barbosa EJ Jr, Gupta NK, Torigian DA, Gefter WB. Current role of imaging in the diagnosis and management of pulmonary hypertension. AJR Am J Roentgenol 2012;198(6):1320–1331.
51. Jenkins DP, Madani M, Mayer E, et al. Surgical treatment of chronic thromboembolic pulmonary hypertension. Eur Respir J 2013;41(3):735–742.
52. Wittram C, Kalra MK, Maher MM, Greenfield A, McLoud TC, Shepard JA. Acute and chronic pulmonary emboli: angiography-CT correlation. AJR Am J Roentgenol 2006;186(6 suppl 2):S421–S429.
53. King MA, Ysrael M, Bergin CJ. Chronic thromboembolic pulmonary hypertension: CT findings. AJR Am J Roentgenol 1998;170(4):955–960.
54. Devaraj A, Hansell DM. Computed tomography signs of pulmonary hypertension: old and new observations. Clin Radiol 2009;64(8):751–760.
55. Agarwal PP, Wolfsohn AL, Matzinger FR, Seely JM, Peterson RA, Dennie C. In situ central pulmonary artery thrombosis in primary pulmonary hypertension. Acta Radiol 2005;46(7):696–700.
56. Peña E, Dennie C, Veinot J, Muñiz SH. Pulmonary hypertension: how the radiologist can help. RadioGraphics 2012;32(1):9–32.
57. Aviram G, Cohen D, Steinvil A, et al. Significance of reflux of contrast medium into the inferior vena cava on computerized tomographic pulmonary angiogram. Am J Cardiol 2012;109(3):432–437.
58. Gluecker T, Capasso P, Schnyder P, et al. Clinical and radiologic features of pulmonary edema. RadioGraphics 1999;19(6):1507–1531; discussion 1532–1533.
59. Staub NC. Pulmonary edema: physiologic approaches to management. Chest 1978;74(5):559–564.
60. Fujii T, Nakamura T, Iwamoto A. Pneumocystis pneumonia in patients with HIV infection: clinical manifestations, laboratory findings, and radiological features. J Infect Chemother 2007;13(1):1–7.
61. Hansell DM. Small-vessel diseases of the lung: CT-pathologic correlates. Radiology 2002;225(3):639–653.
62. Nishino M, Itoh H, Hatabu H. A practical approach to high-resolution CT of diffuse lung disease. Eur J Radiol 2014;83(1):6–19.
63. Cheah FK, Sheppard MN, Hansell DM. Computed tomography of diffuse pulmonary haemorrhage with pathological correlation. Clin Radiol 1993;48(2):89–93.
64. Tomiyama N, Müller NL, Johkoh T, et al. Acute parenchymal lung disease in immunocompetent patients: diagnostic accuracy of high-resolution CT. AJR Am J Roentgenol 2000;174(6):1745–1750.
65. Lara AR, Schwarz MI. Diffuse alveolar hemorrhage. Chest 2010;137(5):1164–1171.
66. de Prost N, Parrot A, Picard C, et al. Diffuse alveolar haemorrhage: factors associated with in-hospital and long-term mortality. Eur Respir J 2010;35(6):1303–1311.
67. Ioachimescu OC, Stoller JK. Diffuse alveolar hemorrhage: diagnosing it and finding the cause. Cleve Clin J Med 2008;75(4):258, 260, 264–265 passim.
68. Peyrol S, Cordier JF, Grimaud JA. Intra-alveolar fibrosis of idiopathic bronchiolitis obliterans-organizing pneumonia: cell-matrix patterns. Am J Pathol 1990;137(1):155–170.
69. Ujita M, Renzoni EA, Veeraraghavan S, Wells AU, Hansell DM. Organizing pneumonia: perilobular pattern at thin-section CT. Radiology 2004;232(3):757–761.
70. Murata K, Khan A, Herman PG. Pulmonary parenchymal disease: evaluation with high-resolution CT. Radiology 1989;170(3 Pt 1):629–635.
71. Frazier AA, Franks TJ, Mohammed TL, Ozbudak IH, Galvin JR. Pulmonary veno-occlusive disease and pulmonary capillary hemangiomatosis. RadioGraphics 2007;27(3):867–882.
72. Lantuéjoul S, Sheppard MN, Corrin B, Burke MM, Nicholson AG. Pulmonary veno-occlusive disease and pulmonary capillary hemangiomatosis: a clinicopathologic study of 35 cases. Am J Surg Pathol 2006;30(7):850–857.
73. Resten A, Maître S, Humbert M, et al. Pulmonary arterial hypertension: thin-section CT predictors of epoprostenol therapy failure. Radiology 2002;222(3):782–788.
74. Swensen SJ, Tashjian JH, Myers JL, et al. Pulmonary venoocclusive disease: CT findings in eight patients. AJR Am J Roentgenol 1996;167(4):937–940.
75. Kligerman SJ, Groshong S, Brown KK, Lynch DA. Nonspecific interstitial pneumonia: radiologic, clinical, and pathologic considerations. RadioGraphics 2009;29(1):73–87.
76. Lee JW, Lee KS, Lee HY, et al. Cryptogenic organizing pneumonia: serial high-resolution CT findings in 22 patients. AJR Am J Roentgenol 2010;195(4):916–922.
77. Silva CI, Müller NL, Lynch DA, et al. Chronic hypersensitivity pneumonitis: differentiation from idiopathic pulmonary fibrosis and nonspecific interstitial pneumonia by using thin-section CT. Radiology 2008;246(1):288–297.
78. Devouassoux G, Cottin V, Lioté H, et al. Characterisation of severe obliterative bronchiolitis in rheumatoid arthritis. Eur Respir J 2009;33(5):1053–1061.
79. Brown KK. Rheumatoid lung disease. Proc Am Thorac Soc 2007;4(5):443–448.
80. Krishnam MS, Suh RD, Tomasian A, et al. Postoperative complications of lung transplantation: radiologic findings along a time continuum. RadioGraphics 2007;27(4):957–974.
81. Nassar AA, Jaroszewski DE, Helmers RA, Colby TV, Patel BM, Mookadam F. Diffuse idiopathic pulmonary neuroendocrine cell hyperplasia: a systematic overview. Am J Respir Crit Care Med 2011;184(1):8–16.
82. Gorshtein A, Gross DJ, Barak D, et al. Diffuse idiopathic pulmonary neuroendocrine cell hyperplasia and the associated lung neuroendocrine tumors: clinical experience with a rare entity. Cancer 2012;118(3):612–619.
83. Davies SJ, Gosney JR, Hansell DM, et al. Diffuse idiopathic pulmonary neuroendocrine cell hyperplasia: an underrecognised spectrum of disease. Thorax 2007;62(3):248–252.
84. Kanne JP, Yandow DR, Meyer CA. Pneumocystis jiroveci pneumonia: high-resolution CT findings in patients with and without HIV infection. AJR Am J Roentgenol 2012;198(6):W555–W561.
85. Arakawa H, Niimi H, Kurihara Y, Nakajima Y, Webb WR. Expiratory high-resolution CT: diagnostic value in diffuse lung diseases. AJR Am J Roentgenol 2000;175(6):1537–1543.
86. Mastora I, Remy-Jardin M, Sobaszek A, Boulenguez C, Remy J, Edme JL. Thin-section CT finding in 250 volunteers: assessment of the relationship of CT findings with smoking history and pulmonary function test results. Radiology 2001;218(3):695–702.